AD 270 181

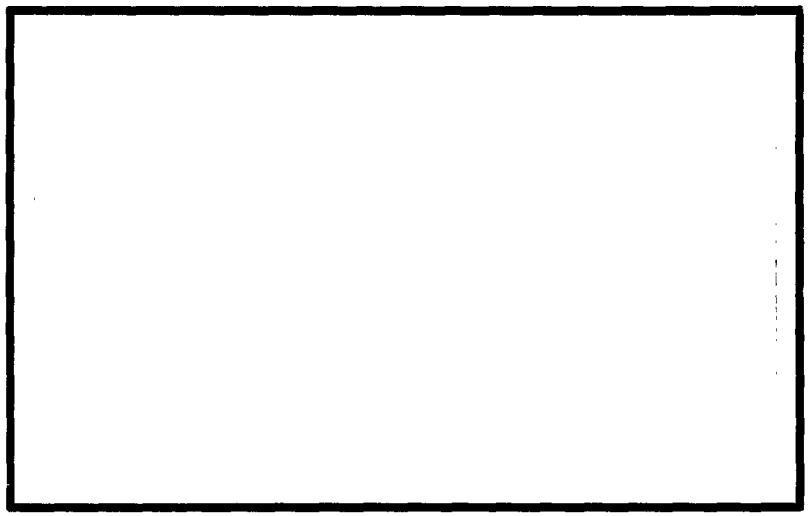

DEPARTMENT OF ELECTRICAL ENGINEERING
UNIVERSITY OF UTAH
SALT LAKE CITY, UTAH

Physics Division, Air Force Office of Scientific Research
ARDC, Washington 25, D. C.
AFOSR No. 1939
ASTIA Doc. No.
Contract No. AF 49(638)-462
Division File No. 1-3-2

A LABORATORY INVESTIGATION OF METEOR PHYSICS

James R. Jensen and E. P. Palmer

15 October 1961

Technical Report OSR-22

High-Velocity Laboratory
Department of Electrical Engineering
University of Utah
Salt Lake City, Utah

ACKNOWLEDGMENTS

The authors wish to acknowledge the help of all members of the High-Velocity Laboratory staff in the accomplishment of the work reported here, in particular, the work of Reed M. Gardner in designing and building the spray-particle detection equipment and collecting preliminary data.

ABSTRACT

The equations of motion for a single particle traveling in a constant density atmosphere are derived. The aerodynamic drag on the particle and the atmosphere-particle energy transfer resulting in loss of particle mass are considered in the derivations. It is assumed as an initial condition that steady-state ablation is occurring. The equations are solved using a Datatron 205 Digital Computer, and the solutions are discussed in some detail. Emphasis is placed on determining particle size and absolute luminosity from measurements of distance versus time.

Micron-size particles, which travel at velocities in lower meteor range of 10 to 20 km/sec, are produced by impact of spherical steel pellets on a steel target. Preliminary experiments were conducted using these particles in a controlled atmosphere. The particles, being luminous, were detected by photomultiplier tubes. The leading edge of a cloud of particles was detected and velocities up to 15 km/sec were measured. By applying the theory to deceleration measurements, the size of the particles was estimated at approximately 1.0 micron diameter.

An improved vacuum firing range was designed to correct for the vacuum and size limitations of the original system. An experiment is proposed to utilize the improved system to detect and measure individual particles. Data from the experiments can be compared with theory and the results applied directly to determine in detail the physical phenomena occurring in meteor flight.

TABLE OF CONTENTS

I. INTRODUCTION

The physical theory of meteors apparently had its beginnings in 1922 and 1923 in the work of Öpik[1] and Lindemann and Dobson.[2] Since that time the theory has been expanded and considerable observational data have been collected. Reports of original work and summaries of the work of others are given by Hoppe[3], Whipple[4], and Hansen[5]. The most complete and the most recent investigations of the physics of meteor flight have been made by Öpik[6] and Levin.[7].

The question naturally arises as to why studies are being made of meteor phenomena and why they are important. The first investigations were carried out as a matter of curiosity as to the nature of meteors and as a means of investigating the upper atmosphere. In recent years the development of earth satellites and space vehicles has made the presently available knowledge of meteors extremely important and is creating an ever increasing demand for further insight into every facet of meteor flight.

Present meteor theory is based on assumptions as to the actual physical processes occurring. Heat transfer to a vaporizing surface, ablation of the surface, and the production of luminosity are not completely understood. As a result, only order-of-magnitude estimates can be given for the size of meteoroid producing a given visual effect. Controlled laboratory experiments are a necessity before the problems of meteor physics can be considered solved.

This paper presents a study of the equations of motion of micron-size particles traveling at meteor speeds in a controlled atmosphere. The relations between size, velocity, distance traversed, and luminosity of the particles are examined. A preliminary experimental investigation is reported and recommendations are made for future studies. Any information gained from these studies can be applied directly to actual meteor problems.

High velocity particles used in the experimental work are produced by shooting a projectile from a gun into a target. As a result of the impact, a cloud of tiny particles is produced which travels away from the target at velocities over five times that of the primary projectile. These particles, henceforth to be referred to as spray particles, are very similar to micro-meteors in both size and velocity, being approximately 1/10 to 10 microns in diameter and traveling between 5 and 20 km/sec.[8, 9]. Spray particles can thus be considered to be experimental meteors and can be studied as such. It is assumed here that a single particle can be separated from the cloud and studied as an individual micrometeorite.

II. THE EQUATIONS OF MOTION OF AN ABLATING PARTICLE

Derivation of Equations

If equations are to be derived to describe a problem that is to be tested experimentally, they must be in terms of experimentally measurable quantities. In spray particle studies, time of flight and distance traveled are easily measured; therefore, it is important that an equation relating these two parameters be determined.

Let it be assumed as a first consideration that the high velocity particle is not losing mass, but is simply being decelerated by the atmospheric resistance to its motion. With the particle as the center of the frame of reference, the mass of air swept up per unit time is $\rho\sigma v$, resulting in a time rate of change of momentum of $\rho\sigma v^2$, where ρ is the density of the atmosphere, σ is the average cross sectional area normal to the direction of motion, and v is the particle velocity measured in the laboratory reference frame. The decelerating force on the particle, $m \frac{dv}{dt}$, can be related to the change in momentum by the factor C_D, the drag coefficient, which accounts for the efficiency of the momentum exchange process. The drag equation is

$$m \frac{dv}{dt} = -1/2\ C_D\ \rho\sigma v^2 \qquad (1)$$

Equation (1) can be integrated to obtain velocity.

$$\int_{v_o}^{v} \frac{dv}{v^2} = -\int_{o}^{t} \beta\ dt, \qquad \beta = \frac{\rho\sigma C_D}{2m}$$

thus $$\frac{1}{v} - \frac{1}{v_o} = \beta t,$$

and $$v = \frac{v_o}{\beta v_o t + 1} \qquad (2)$$

where v_o is the initial velocity of the particle at the time it is created. The distance traveled is then

$$x = \int_o^t v dt = \int_o^t \frac{v_o}{\beta v_o t + 1} dt$$

Performing the integration,

$$x = \frac{1}{\beta} \ln (1 + \beta v_o t). \qquad (3)$$

Assuming that the particles are approximately spherical in shape,

$$\beta = \frac{\rho o C_D}{2m} = \frac{\rho \pi r^2 C_D}{2(4/3 \pi r^3 \delta)} = \frac{3}{8} \frac{\rho C_D}{r \delta}, \qquad (4)$$

where δ is the density of the particle and r is its radius. Equation (3) generates a family of trajectory curves, so that by changing β the various members of the family are obtained. β is a function of the four parameters ρ, C_D, δ, and r. For experiments in a controlled atmosphere, ρ and δ are known leaving only C_D/r as an unknown. For elastic or completely-inelastic collisions between meteor and air molecules in free molecular flow, $C_D = 2$. (A more complete discussion of C_D is given later.) The curves generated by Eq. (3) are therefore only a function of particle size. An experiment can be performed to find time of flight at various distances. These values can be plotted and the resulting curve compared with those of Eq. (3) to determine particle size.

Results obtained from the above equations would be in error, since the particles are known to be luminous and therefore must be ablating. Consider a particle traveling with a velocity v through a medium of constant density ρ. Again using the particle as the center of the reference frame, the mass of air that is intercepted per unit time is $\sigma\rho v$, where σ is the cross-sectional area normal to the direction of motion. The kinetic energy swept up per unit time, $(\frac{dE}{dt})$, is $\frac{1}{2}\sigma\rho v^3$. If a fraction γ of this energy goes into ablating the particle, then

$$\gamma \frac{dE}{dt} = \gamma \left(\tfrac{1}{2}\sigma\rho v^3\right) = - h \frac{dm}{dt} ,$$

and

$$\frac{dm}{dt} = - \frac{1}{2} \frac{\gamma\sigma\rho v^3}{h} , \tag{5}$$

where m is the instantaneous mass of the particle and h is the heat of ablation.

The drag on the particle is given by

$$m \frac{dv}{dt} = - \frac{1}{2} C_D \sigma\rho v^2 . \tag{1}$$

The deceleration is

$$\frac{dv}{dt} = - \frac{1}{2} \frac{C_D\sigma\rho v^2}{m} . \tag{6}$$

Time can be eliminated by dividing Eq. (5) by Eq. (6).

$$\frac{dm}{dt} = \frac{\gamma m v}{h C_D}$$

or

$$\frac{dm}{m} = \frac{\gamma}{h\, C_D} v dv \tag{7}$$

If the particles are assumed to be spherical, which is a good supposition since the particles are small, probably molten, and more than likely rotating which tends to smooth out irregularities, the mass of a particle of density δ is

$$m = \frac{4}{3}\pi r^3 \delta \ ,$$

so

$$\frac{dm}{m} = \frac{4\pi r^2 \delta dr}{4/3\pi r^3 \delta} = 3\,\frac{dr}{r} \tag{8}$$

Substitution in Eq. (7) gives

$$\frac{dr}{r} = \frac{1}{3}\,\frac{\gamma}{hC_D}\,vdv \tag{9}$$

Integration of both sides of Eq. (9) results in

$$\ln\left(\frac{r}{r_o}\right) = k\,(v^2 - v_o^2)$$

and

$$r = r_o \epsilon^{-k\,(v_o^2 - v^2)} \ , \tag{10}$$

where $k = \frac{1}{6}\,\frac{\gamma}{hC_D}$ and r_o and v_o are initial values. Equation (6) can now be rewritten in terms of the size of the particle.

$$\frac{dv}{dt} = -\frac{1}{2}\,\frac{C_D \sigma \rho v^2}{m} = -\frac{1}{2}\,\frac{C_D(\pi r^2)\rho v^2}{4/3\pi r^3 \delta} = -\frac{3}{8}\,\frac{C_D \rho}{r\delta}\,v^2$$

Substituting the value of r from Eq. (10),

$$\frac{dv}{dt} = -\frac{3}{8}\frac{C_D\rho}{r_o\delta} v^2 \epsilon^{-k(v^2 - v_o^2)} = -\frac{3}{8}\alpha_o v^2 e^{-k(v^2 - v_o^2)} \tag{11}$$

where $\alpha_o = \frac{C_D\rho}{r_o\delta}$.

It will be later found that the luminosity is directly proportioned to the time rate of change of mass, so it will be convenient to have an equation for $\frac{dm}{dt}$. Again assuming a spherical particle

$$m = \frac{4}{3}\pi r^3\delta$$

and

$$\frac{dm}{dt} = 4\pi r^2\delta \frac{dr}{dt} \tag{12}$$

From Eq. 10

$$\frac{dr}{dt} = 2kvr \frac{dv}{dt} \tag{13}$$

Combining Eqs. (11), (12), and (13)

$$\frac{dm}{dt} = 3\pi k C_D\rho r^2 v^3. \tag{14}$$

With the previously derived equations, the luminosity can now be calculated in terms of experimentally measureable quantities. The intensity of luminous radiation is usually assumed to be given by [10]

$$I = -\frac{\tau}{2}\frac{dm}{dt} v^2 \tag{15}$$

where τ is the luminous efficiency. The actual processes involved in producing the visible radiation are complicated and can not be given accurately by the simple relationship above; however, the simple equation seems to suffice to describe the essential features of the phenomenon.[5] Observational evidence indicates that the luminous efficiency will not be constant but will vary approximately linearly with the velocity[5,10,11] so that

$$\tau = \tau_o v \quad .$$

Therefore,

$$I = - \frac{\tau_o}{2} \frac{dm}{dt} v^3 \quad . \tag{16}$$

Substitution of Eq. (14) results in

$$I = \frac{3}{2}\pi k \, C_D \, \rho \tau_o r^2 v^6 \tag{17}$$

Evaluation of Equation Parameters

Many of the parameters in the equations of motion of an ablating particle will be either constant or restricted to a certain range in any experiments that can be performed. It is thus important that values or ranges of values be determined for these parameters.

The experiments will be conducted in a vacuum tank which means that the atmospheric density inside the tank can be controlled. The range of values for ρ will thus depend on the pressures that can be obtained in a firing range. Most meteor phenomena occur in regions of the atmosphere where the mean free path is large compared to the meteor body. For the easily obtainable pressure range of 0.1 mm Hg. to 10 mm Hg.

the mean free path is about 5 to 500 microns which is of the same magnitude or larger than the micron-sized particles that will be studied. Thus for preliminary investigations, the range of pressures used will be 0.1 mm Hg. to 10 mm Hg. or in terms of density $\rho = 8 \times 10^{-8}$ g/cm^3 to 1.5×10^{-5} g/cm^3.

To simulate iron-nickle meteors, the first experiments may be conducted by shooting steel balls into steel targets. The density of the spray particles will therefore be that of steel, so $\delta = 7.8$ g/cm^3.

Previous spray particle work[8,9] has shown that initial velocities up to 20 km/sec are present. This is well within the meteor velocity range of 11 to 73 km/sec. The range of values that will be used in the equations is 10 to 20 km/sec. Previous work has also shown that the particles range in size between 0.1 microns and 10 microns in diameter. These values will be used for r_o in the equations.

The coeficient of drag to be used in the equations has been the object of much study. Baker[12] concluded that the molecules that are thermally emitted from a high velocity object have a profound effect upon the drag and cannot legitimately be neglected. Baker and Charwat[12] found that by incorporating the behavior of the emitted molecules into the analysis of a sphere, that a more realistic drag coefficient for a sphere has the form

$$C_D = 2 \left| 1 - D_1 B + (E_0 + E_1 B) \frac{\bar{V}_e}{\dot{y}} \right. \quad , \tag{18}$$

where B equals the ratio of the diameter of the sphere to the mean free path of the emitted molecules with respect to the oncoming molecules;

$\overline{V_e}$ is the average speed of the emitted molecules, $\dot{y}$ is the speed of the object; $D_1 = 0.23$, $E_o = 0.444$, and $E_1 = 0.65$.

Another theory[13] claims the possibility that the drag coefficient is a function of velocity, giving for the drag force.

$$F_D = -\frac{1}{2} C_D \rho v^2 \overline{\sigma} \left[1 + 0.16s \frac{\gamma}{\frac{1}{2}C_D}\right] \tag{19}$$

Here v is the velocity of the high speed object, γ is the heat transfer coefficient, and s the object velocity in units of 10 km/sec. Using this equation drag is increased by a factor of one-half for a velocity of 30 km/sec and is doubled at 60 km/sec.

C_D, the drag coefficient, is a function of the thickness of the shock layer or cushion of air that appears at the front of the moving object, and also of the shape of the object. All sources agree, however, that when the meteor is small (in the micron range) the air cap is non-existent or negligible, the shape is unimportant and the effects of the thermally emitted molecules are small. Thus the drag coefficient takes on a value of approximately two. Since the particles that are to be studied here are of the order of a few microns, it will be assumed that C_D is exactly equal to two.

The coefficient of heat transfer, γ, is equal to the coefficient of accommodation, K, when there is no air or vapor cap to shield the high velocity particle from oncoming air molecules. The accommodation coefficient is equal to the fraction of the kinetic energy of air lost in the collision process. Let it be assumed that v is the velocity of

the oncoming air molecules and v' is the velocity of the reflected molecules both measured relative to the particle. The kinetic energy lost by the air molecules in the collision is

$$= \frac{\frac{1}{2}\mu v^2 - \frac{1}{2}\mu v'^2}{\frac{1}{2}\mu v'^2} = 1 - \left(\frac{v'}{v}\right)^2 \qquad (20)$$

where μ is the mass of a molecule of air. The accommodation coeficient is therefore only dependent on the incident and reflected velocities of the air molecules. If the air molecules are totally reflected, $v' = -v$ and $\kappa = 0$; if the air molecules stick to the particle, $v' = 0$ and $\kappa = 1$. It is pointed out by Öpik[6] that if a vapor or air layer is present γ may differ considerably from κ, however, for this study of micron-size particles the air cap is negligible and $\gamma = \kappa$. Since it is doubtful that the air molecules will be completely reflected or will stick, a range of γ will be chosen within the maximum values. γ will be assumed to be between 0.3 and 0.9. A theoretical discussion of κ can be found in Öpik[6], and a discussion based on experimental investigation of κ is given by Hansen[5].

The heat of ablation, h, can vary over a wide range and is a direct result of what type of process is responsible for ablation. For a high speed particle, ablation may be by vaporization, fusion and spraying of the liquid, sputtering, fragmentation, and by a combination of any or all of these processes.[6]

Sputtering, which unlike vaporization does not depend on temperature, is a process whereby the impact of high-speed atomic particles may knock out single atoms from a solid or liquid surface. Sputtering seems to be unimportant except for very high velocity particles (50-80 km/sec)[14].

The heats of ablation for the various processes can be estimated by using the following values for iron given by Öpik[6].

Physical Properties of Iron

Melting Point	1800° K
Boiling Point	3508° K
Average Specific Heats	
Solid	6.91×10^6 erg/g°C
Liquid	6.66×10^6 erg/g°C
Gas	$C_v = 2.23 \times 10^6$ erg/g°C
	$C_p = 3.72 \times 10^6$ erg/g°C
Latent Heat of Fusion	2.69×10^9 erg/g
Latent Heat of Vaporization	6.40×10^{10} erg/g

The heat of ablation for melting and spraying, h_f, assuming an initial temperature of 283° K is

$$h_f = 6.91 \times 10^6 \frac{\text{erg}}{\text{g°C}} \quad (1800\text{-}283)\text{°C} + 2.69 \times 10^9 \frac{\text{erg}}{\text{g}} = \quad (1.05 \times 10^{10} +$$

$$0.269 \times 10^{10}) \quad \frac{\text{erg}}{\text{g}} = 1.30 \times 10^{10} \frac{\text{erg}}{\text{g}}.$$

The heat of ablation for vaporization, h_v, is

$$h_v = h_f + 6.66 \times 10^6 \frac{\text{erg}}{\text{g°C}} \quad (3508\text{-}1800)\text{°C} + 6.40 \times 10^{10} \frac{\text{erg}}{\text{g}} = 8.84 \times 10^{10} \frac{\text{erg}}{\text{g}}.$$

The range of values for the heat of ablation is therefore

$$1.3 \times 10^{10} \frac{\text{erg}}{\text{g}} < h < 8.84 \times 10^{10} \frac{\text{erg}}{\text{g}}.$$

From the above discussion, it can be seen that C_D, r, h, k, and α_o will be approximately constant over a limited range of experimental conditions. In integrating the equations of motion, they will be assumed

constant over the range of integration. If it becomes evident that the parameters change significantly during the flight of one particle, a stepwise integration can be performed to approximate the actual change in conditions.

Table I summarizes the parameter values that have been chosen as appropriate for the present study of micron-size particles.

Table I -- Values of parameters to be used in equations of motion.

Pressure	(p)	0.1 - 10 mm H_g
Atm. Density	(ρ)	8×10^{-8} - 1.5×10^{-5} g/cm^3
Particle Density	(δ)	7.8 g/cm^3
Initial Radius	(r_o)	0.05 - 5.0 micron
Initial Velocity	(v_o)	10 - 20 km/sec
Drag Coefficient	(C_D)	2.0
Heat Transfer Coefficient	(γ)	0.3 - 0.9
Heat of Ablation	(h)	10^{10} - 10^{11} erg/g
$k = \frac{\gamma}{6hC_D}$		.0025 - .075 sec^2/km^2
$\alpha_o = \frac{C_D \rho}{r_o \delta}$		.41 x 10^{-2} - 77 m^{-1}

In the solutions of the equations of motion discussed in the next section, it is assumed that the particles have been heated and steady-state ablation conditions attained at the time of initial observation of the flight. A more complete discussion of this requirement will be given in a later report along with extensive calculations of trajectories under a wide range of conditions.

Solution of Equations and Discussion of Results

The equations of motion of an ablating particle may be integrated in terms of exponential integrals to obtain particle size and velocity as a function of distance. This is discussed in Appendix I.

In any experimental work, it is convenient to measure the time taken for a high speed particle to travel a given distance, hence Eq. (11), the expression for the particle's deceleration, must be integrated to arrive at an expression for distance as a function of time. Since the equation is not directly integrable, and numerical methods must be employed, it was decided to use the University of Utah Datatron 205 digital computer to perform the integration. The values of time, velocity, and displacement derived from the deceleration equation can then be used to solve the remaining equations of motion. The computer was programmed to solve for the following quantities: t, v, x, r/r_o, dm/dt and I/τ_o. The program used is discussed in Appendix II.

The manner in which the size of an ablating particle changes with time is shown in Fig. 1 which is a plot of r/r_o versus time for various values of the size parameter $\alpha_o = C_D\rho/r_o\delta$. The curves are drawn for $v_o = 15$ km/sec, $\gamma = 0.6$, $h = 2 \times 10^6$ joules/kg, and $C_D = 2.0$, thus $k = 0.006$ sec^2/km^2. It can be seen that as the value of α_o becomes larger, the rapid decrease in size due to ablation occurs at smaller values of time and therefore also at smaller values of displacement.

It is interesting to note that allof the curves of Fig. 1 have identically the same shape and all reach a leveling-off region at about $r/r_o = 0.25$ where ablation continues at a much slower rate. If a value of r/r_o is known at a given time for one value of α_o, the time at

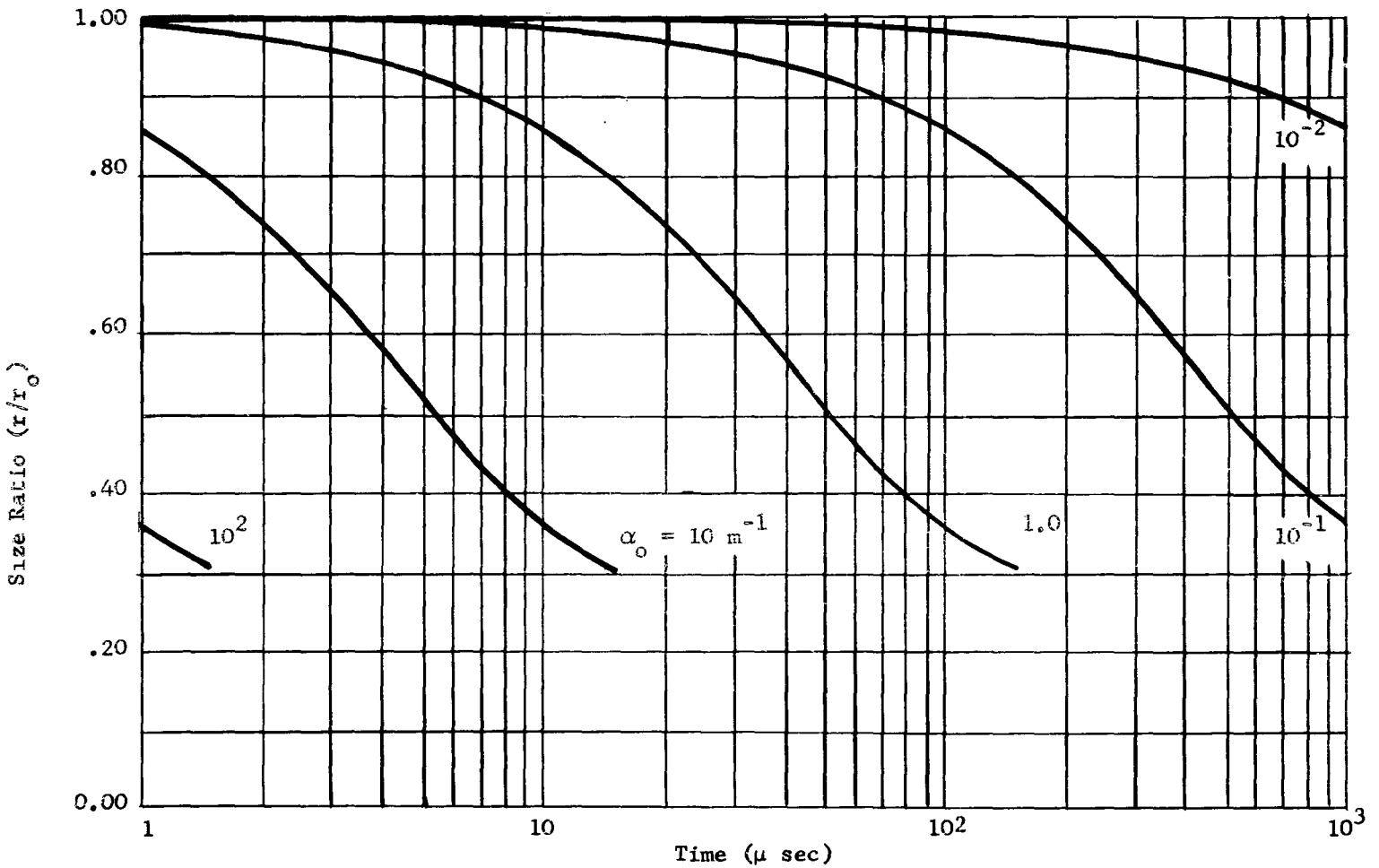

Fig. 1 - Size ratio versus time for an ablating particle for various values of the size parameter $\alpha_o = C_D\rho/r_o\delta$. v_o = 15 km/sec; k = 0.006 sec^2/km^2.

which r/r_o has the same value for another curve is found by multiplying the given time by the ratio of the second value of α_o to the first. This allows a universal curve to be drawn for all values of α_o (v_o and k are constant for each curve). Three of these curves are shown in Fig. 2 for k = 0.006 sec^2/km^2 and three different values of v_o.

Fig. 3 shows the distance traveled by an ablating particle as a function of time. Here again v_o = 15 km/sec and k = 0.006 sec^2/km^2, and the curves are plotted for different values of α_o. In this plot also there is a certain regularity in the shape of the various curves. In this case, to change from one curve to another, the time and displacement coordinates are multiplied by the ratio of the two appropriate values of α_o. This allows a universal curve to be drawn for all values of α_o for given values of v_o and k. Three such curves are shown in Fig. 4 for different values of v_o. For a given value of α_o the curve deviates very little from the curve of constant velocity until the particle radius has been reudced to approximately 70 per cent of its original value. At this time the curve bends away from the others rapidly. It is in this range that the size of a particle can be accurately determined experimentally.

The previous discussion has been limited to specific values of k and v_o. All particles, however, will not have identical ablation rates and initial velocities. It is important in this study of size determination to know how the distance versus time curves are changed by varying these quantities. Figure 5 shows curves for specific values of k and α_o for three initial velocities. It is clear from the figure that for small values of time each curve approaches an asymptote dependent on the

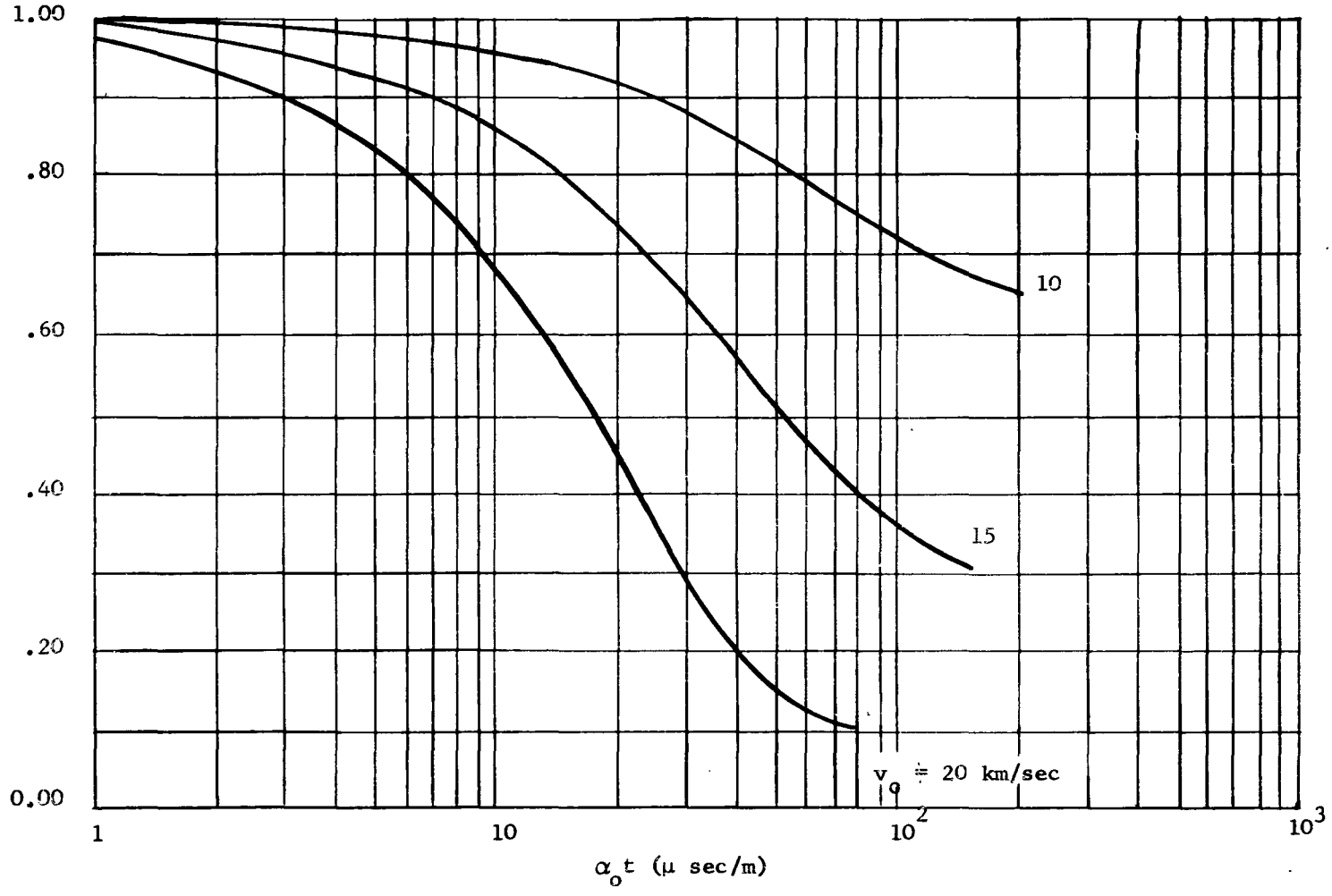

Fig. 2 - Universal curve of size ratio versus time for an ablating particle for various values of initial velocity. $k = 0.006$ sec^2/km^2.

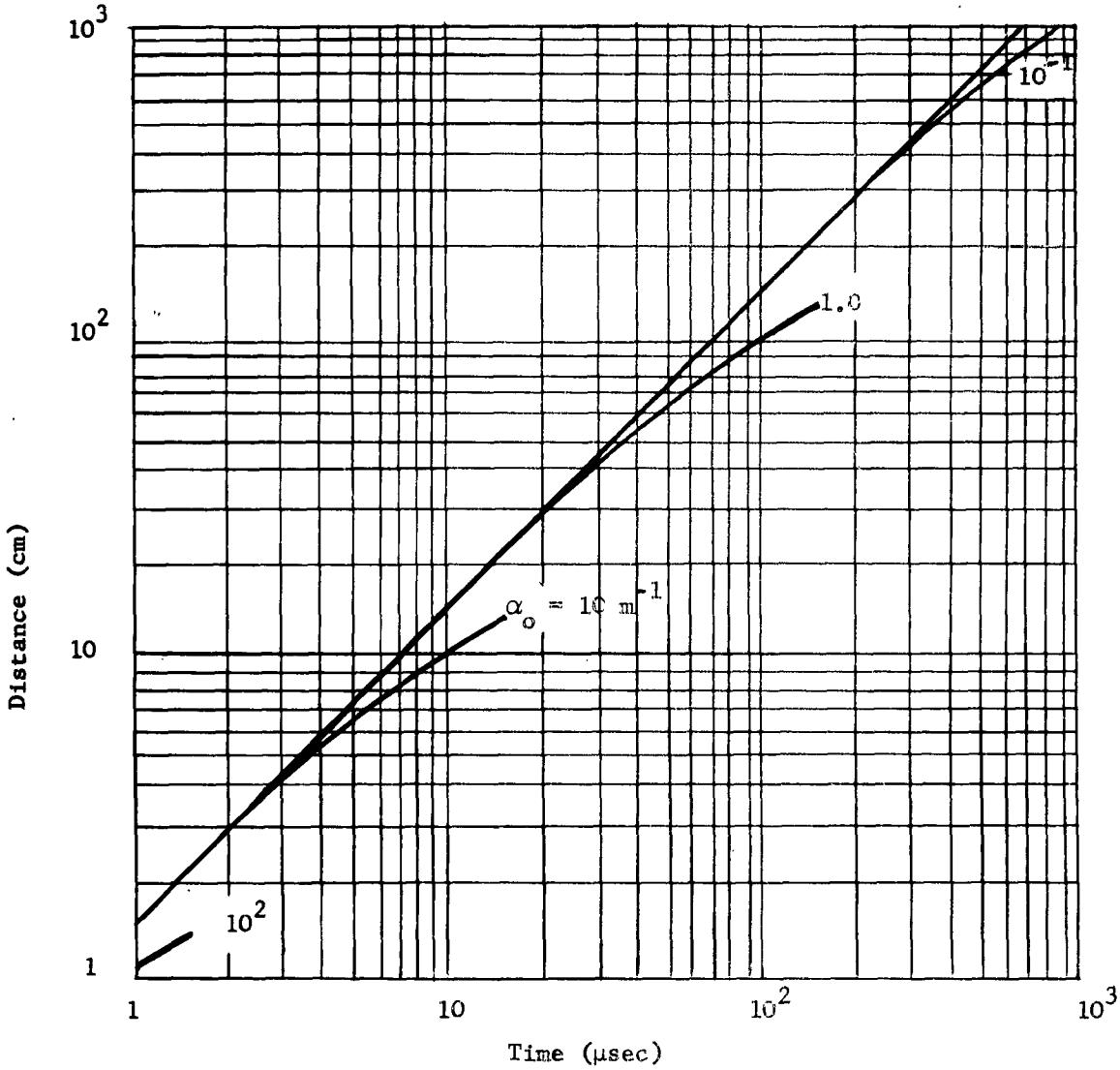

Fig. 3 - Distance versus time for an ablating particle for various values of $\alpha_o = C_D\rho/r_o\delta$. v_o = 15 km/sec; k = 0.006 sec^2/km^2.

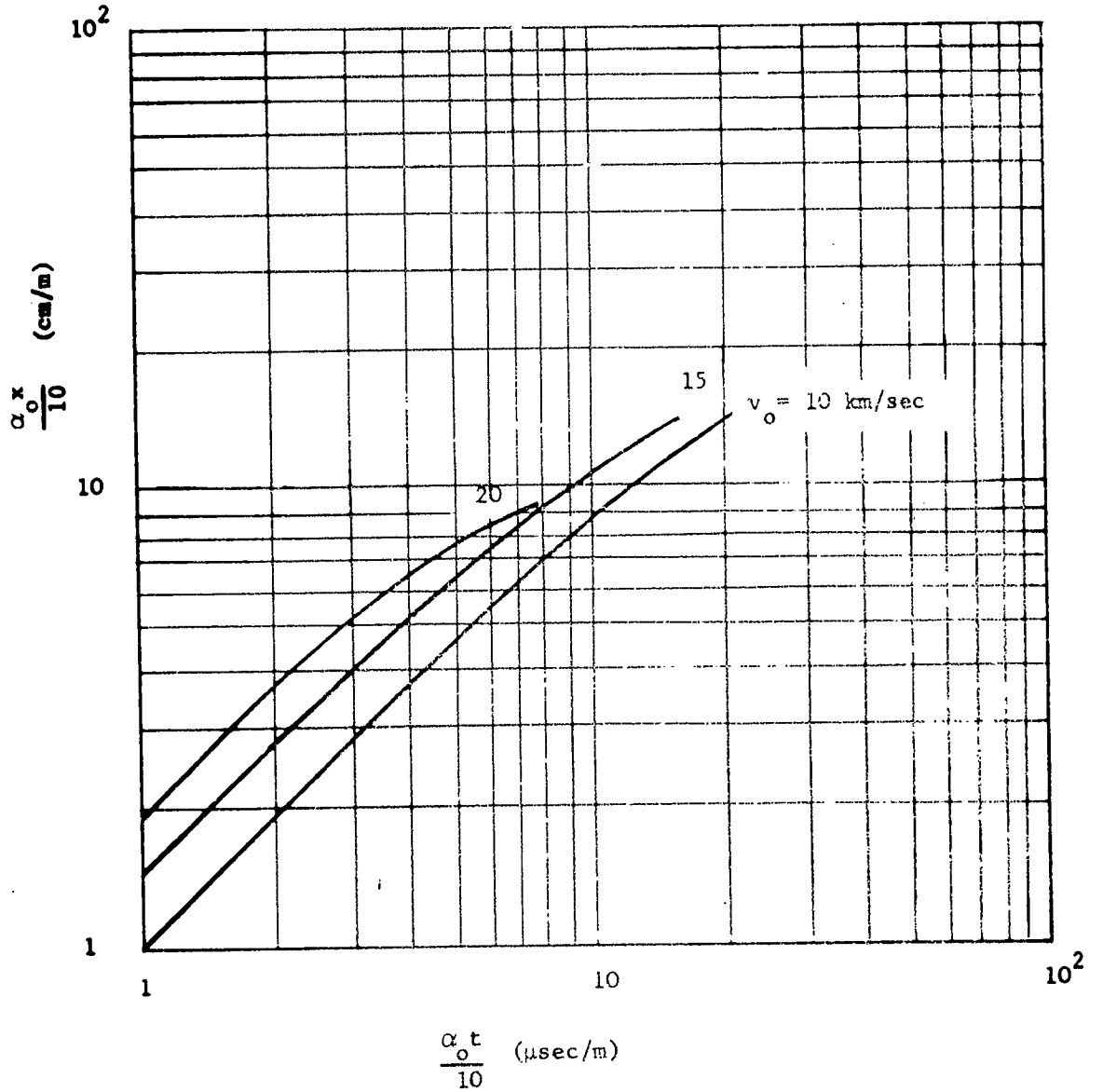

Fig. 4 - Universal Curves of distance versus time for an ablating particle for various values of v_o . k = 0.006 sec^2/km^2.

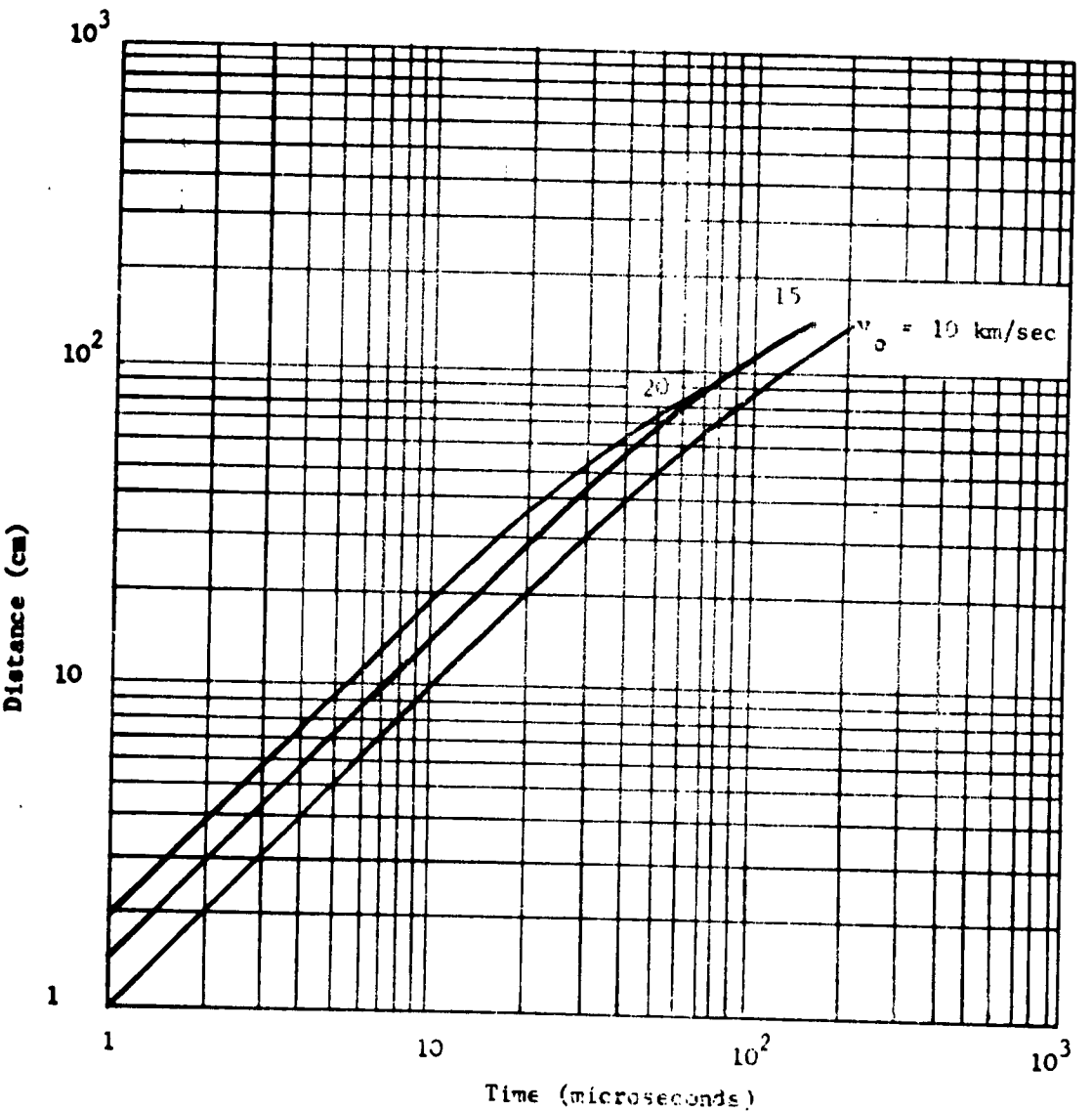

Fig. 5 - Variance in distance versus time curves resulting from a change in initial velocity.

$\alpha_o = 1.0\ m^{-1}$, $k = 0.006\ sec^2/km^2$.

value of v_o. The asymptotes are, of course, just the curves for constant velocities equal to v_o. Experimentally it should not be difficult to determine the initial velocity for a given particle since the deviation from the asymptote in each case occurs in approximately the same distance range but at widely different times. An ideal method of determining initial velocity would be to have a detector placed very close to the target to measure the velocity at this point.

Figures 6, 7, and 8 show the variance in a distance versus time curve for various values of k for initial velocities v_o, of 10, 15 and 20 km/sec. The difference in k arises from different heat transfer coefficients and heats of ablation. The non-ablation case of Eq. 3 is represented by $k = 0$. Ablation by vaporization is shown by the curves for $k = 0.0025$ and $k = 0.006$, and ablation by melting and spraying by $k = 0.05$ in Fig. 6. Since the process of ablation by spraying predominantly occurs with larger particles, values of k over approximately 0.01 $(sec/km)^2$ will not be important with the tiny particles that are of interest in this study.

In the range of k used here, there is a very little difference between the ablating particle and the non-ablating particle for low initial velocities. Depending on the accuracy of experimental work, it may be perfectly all right to determine initial size from the equation for a non-ablating particle. However, when size at a given time is required, the ablation case must be used. For high velocities k becomes more important as shown by Fig. 7 and 8. In the following discussion it will be seen that the value of k is very important in the study of luminosity and will have to be considered.

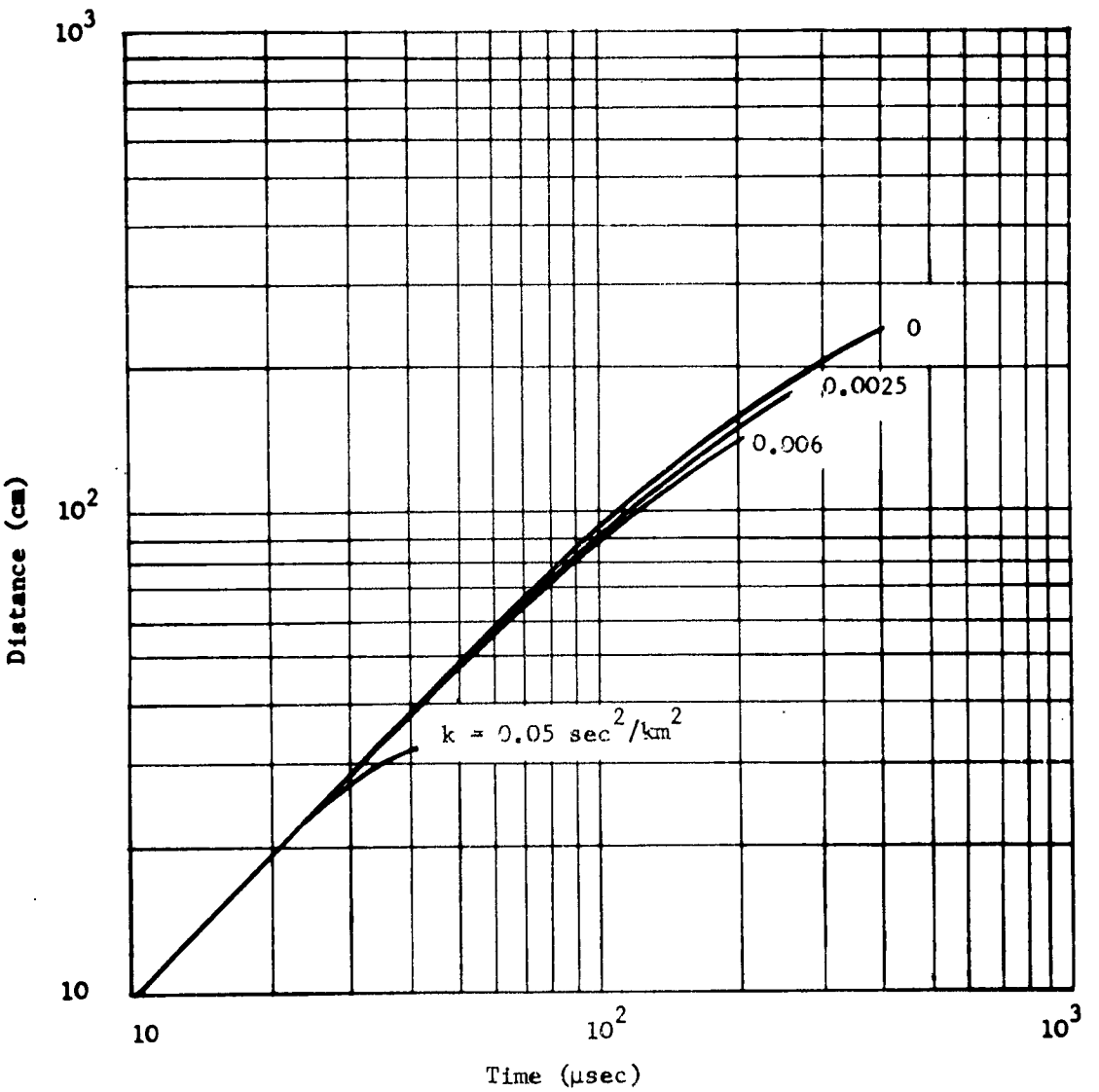

Fig. 6 - Distance versus time curves for an ablating particle for various values of k. α_o = 1.0 m^{-1}; v_o = 10 km/sec.

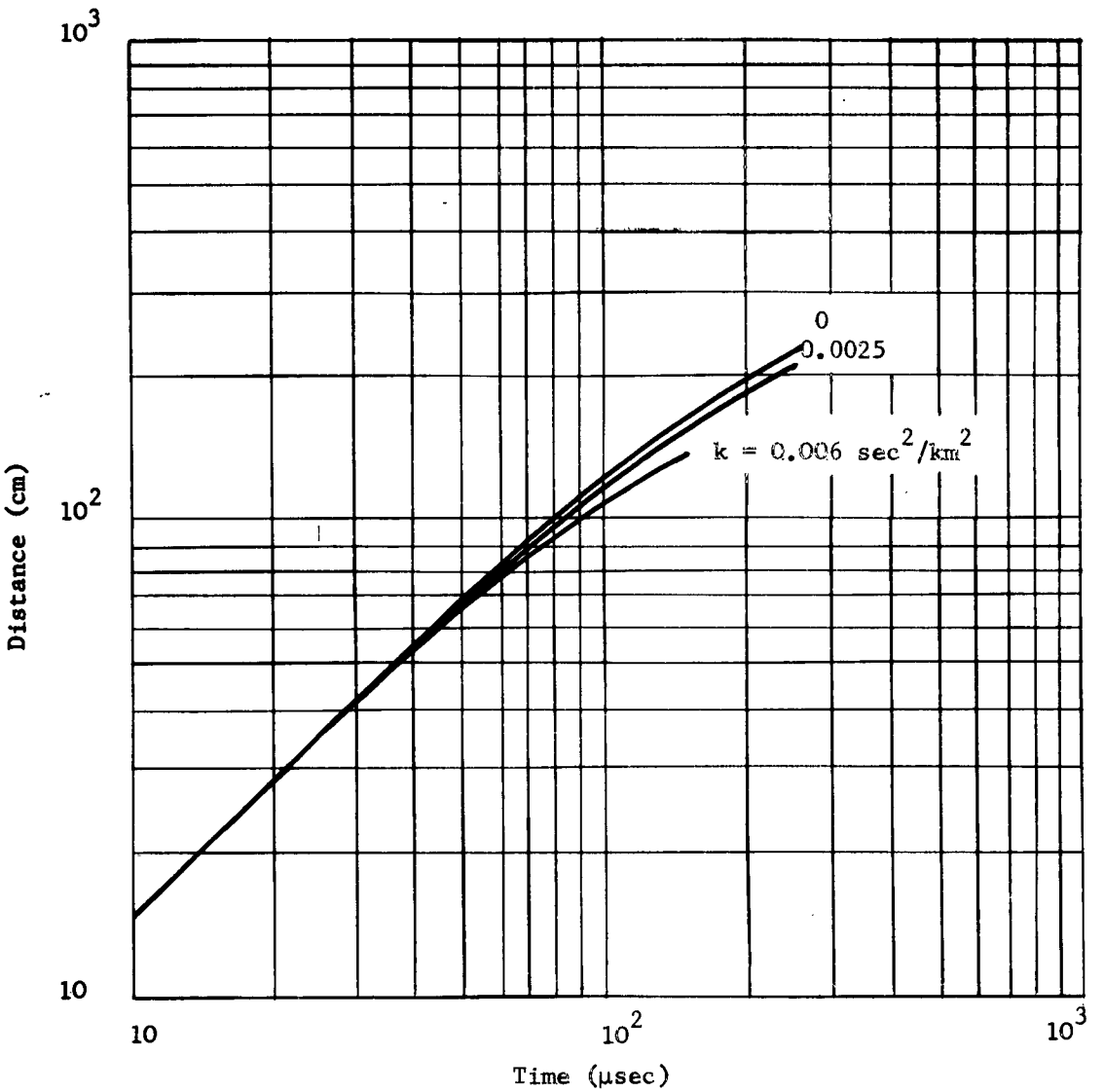

Fig. 7 - Distance versus time curves for an ablating particle for various values of k. $\alpha_o = 1.0\ m^{-1}$; $v_o = 15$ km/sec.

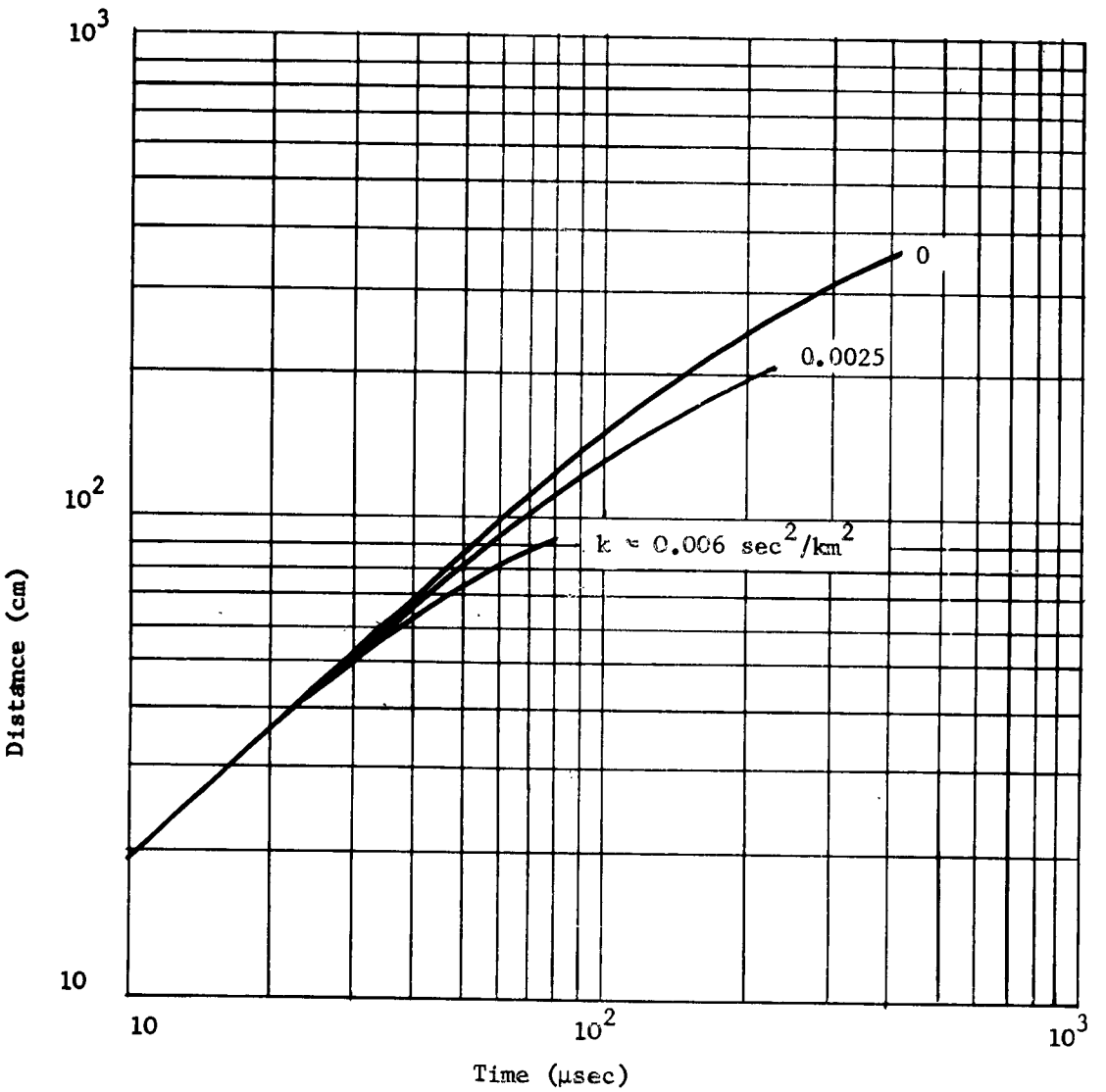

Fig. 8 - Distance versus time for an ablating particle for various values of k. α_o = 1.0 m^{-1}; v_o = 20 km/sec.

The luminosity of a high-speed particle is given by Eq. (17) as

$$I = 3/2\pi k C_D \rho \tau_o r^2 \qquad (17)$$

It was found in programming the computer that the luminous intensity could be obtained more conveniently from the expression

$$\frac{I}{\tau_o C_D \rho r_o^2} = 3/2\pi k \, (r/r_o)^2 \, V^6 \qquad (20)$$

Equation 20, differing only by a constant from Eq. (17), is plotted in Fig. 9 for k = 0.006 $(\text{sec/km})^2$ and v_o = 15 km/sec. The curves show a marked difference for various values of the size parameter α_o; thus, the luminous intensity of a large particle remains constant at its initial value for a much longer time than for a small particle.

As with the curves of Figs. 1 and 3, a universal intensity curve can be drawn. The same intensity for one curve is obtained on another curve by dividing the value of α_o by a given amount and multiplying the time by the same amount. Thus one curve can be drawn for specified values of k and v_o. The intensity curve for any size particle can then be found by multiplying the time scale by the required correction factor. Universal curves are shown in Fig. 10 for different velocities.

Figures 11 and 12 show how the luminous intensity varies with changes in v_o and k. For a given size particle there is a difference in intensity of approximately a factor of 10 when the initial velocity is different by a factor of 5. There is also a progressive increase in the time rate of change of intensity as initial velocity is increased. It can be seen from Fig. 11 that for intensity studies, the initial velocity must be measured

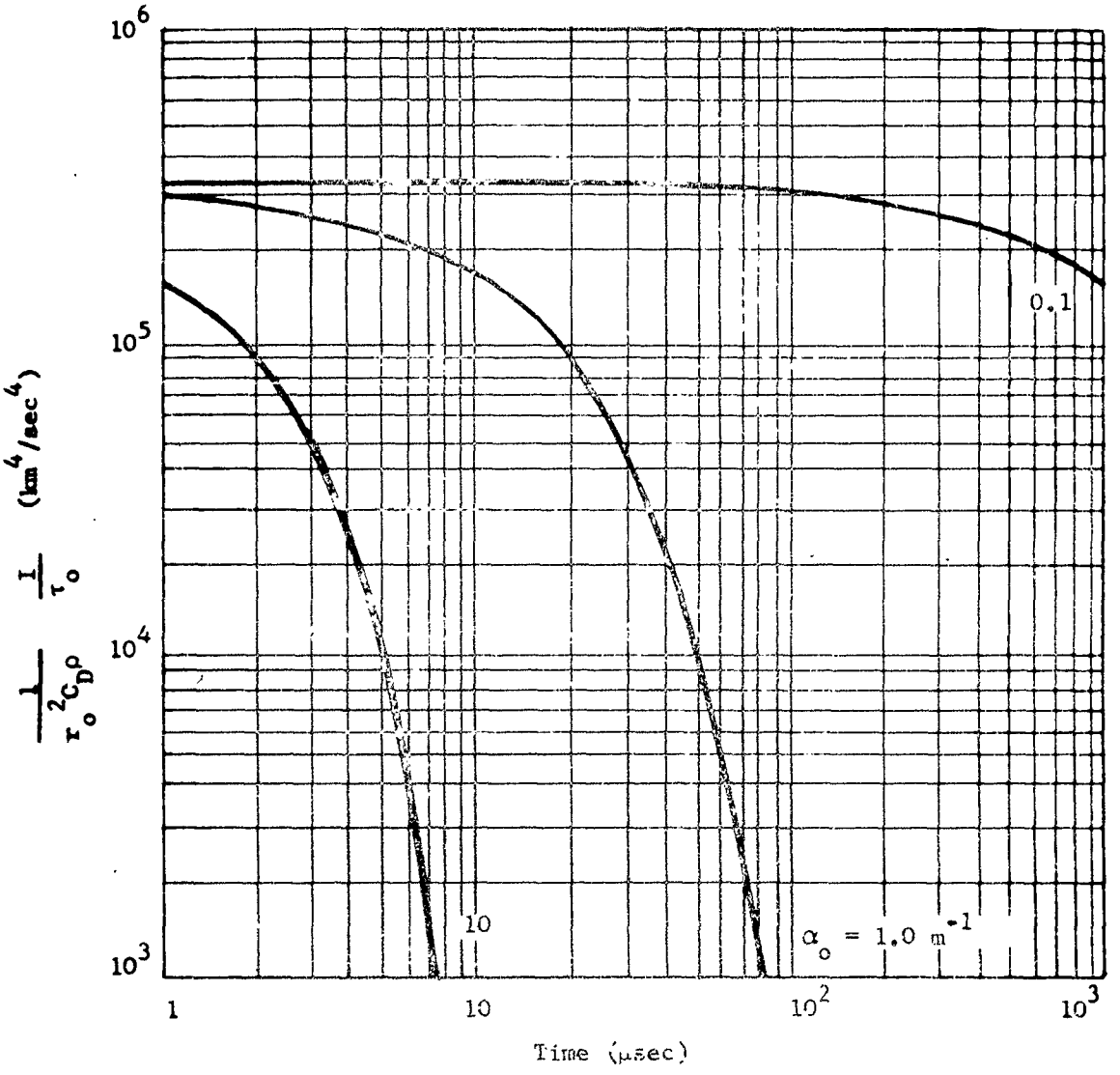

Fig. 9 - Luminous intensity versus time for an ablating particle for various values of $\alpha_o = C_D \rho / r_o \delta$. v_o = 15 km/sec; k = 0.006 sec^2/km^2.

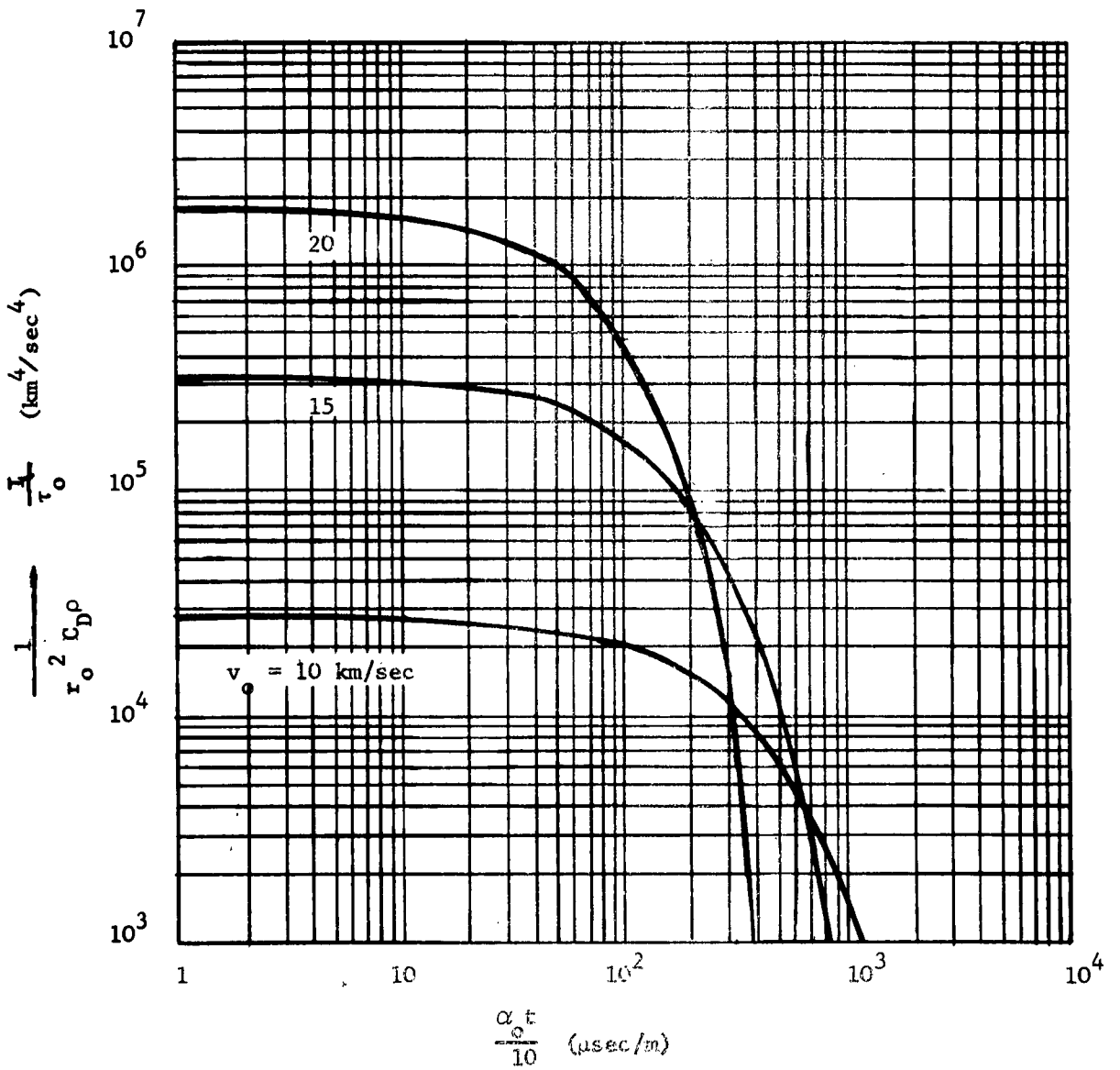

Fig. 10 - Universal luminous intensity curves for an ablating particle for various values of initial velocity. $k = 0.006$ sec^2/km^2.

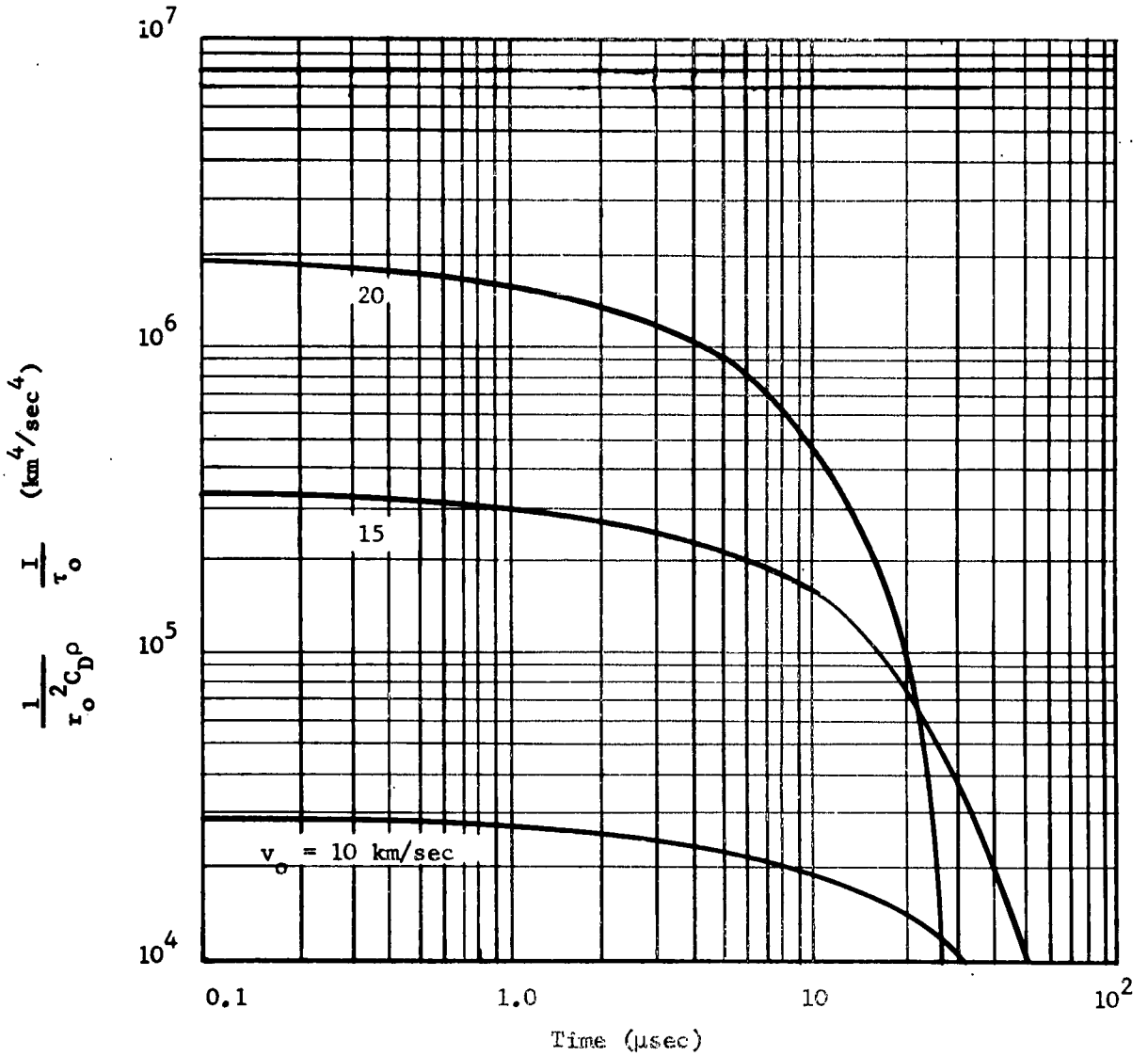

Fig. 11 - Luminous intensity versus time for an ablating particle for various values of initial velocity. $\alpha_o = 1.0\ m^{-1}$; $k = 0.006\ sec^2/km^2$.

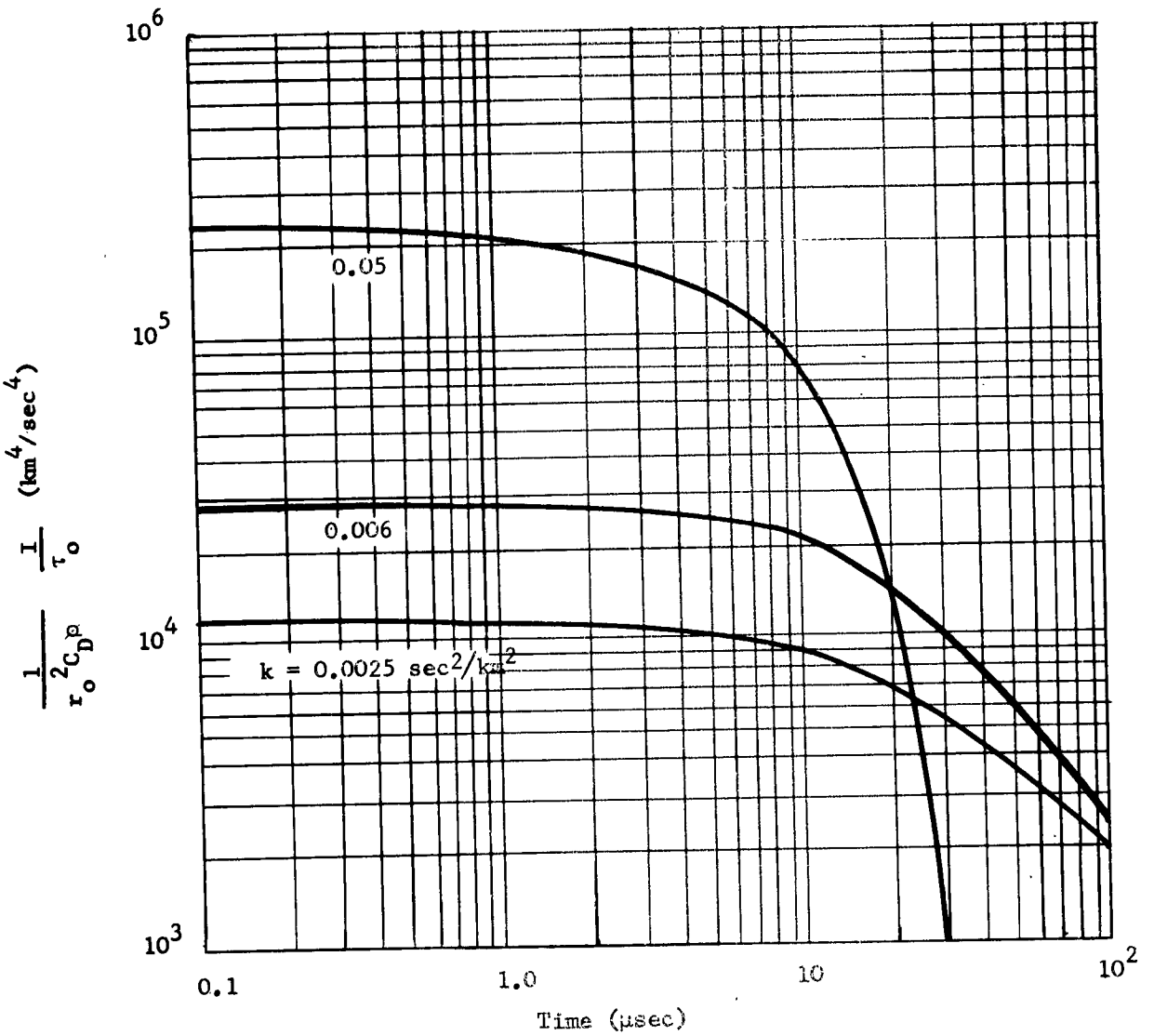

Fig. 12 - Luminous intensity versus time for an ablating particle for various values of k. α_o = 1.0 m^{-1}; v_o = 10 km/sec

experimentally to within at least 1 km/sec before any accurate conclusions can be drawn on luminosity.

The intensity varies with k. The value of k is not easily measured by experiment and so must be calculated on the basis of present knowledge. Assuming the particles are ablating by vaporization, k will have a value close to 0.006 sec^2/km^2. The error in luminosity using k = 0.006 when the actual value is 0.0025 is a factor of about 2.3 based on the curves of Fig. 12. If this amount of inaccuracy can be tolerated a value of k = 0.006 sec^2/km^2 can always be used.

It is possible that the size of high velocity particle size, can be measured by an experiment that measures their luminosity. Since the luminous intensity varies strongly with particle size, an accurate measure of intensity versus time could easily indicate size.

III. EXPERIMENTAL STUDIES OF SPRAY PARTICLES

High-velocity spray particles produced by the impact of a projectile on a target, provide a source of meteor-like particles and allow the laboratory investigation of problems of meteor physics. With these particles, the equations derived in the previous section may be tested and the parameters evaluated.

Earlier work on spray particles by J. S. Clark, R. R. Kadesch, R. W. Grow, W. H. Clark, R. E. Blake, and E. P. Palmer [8,9,15,16] has resulted in the determination of many of the properties of the particles and the development of experimental techniques. In particular, it has been determined that the particles range in size from 1/10 to 10 microns and velocities up to 20 km/sec exist. Unpublished work by R. R. Kadesch indicates that higher velocities may be present and that the smaller particles have the higher velocities. Limitations in the experimental equipment used in the earlier work has limited the investigation to the size and velocity ranges indicated. In all earlier spray particle work, the cloud of particles produced in an impact has been observed as a whole. Velocity measurements have been made of the leading edge of a moving cloud.

The experimental work reported here has been aimed at obtaining individual spray particles with known size and velocity in order to more effectively investigate meteor phenomena and hypervelocity-impact phenomena. Preliminary experimental work will be discussed and the limitations imposed by the equipment used will be considered. An improved firing range, which has been built will be described and proposed experiments in the new range

will be presented.

Design of Experiment to Measure Particle Size

In Section II, the equations of motion of an ablating particle were derived and solved. The next step is to obtain experimental data to compare with the theoretical work.

Spray particles are luminous; therefore, a light sensing device can be used to detect the particles as they pass, and a series of these detectors, together with appropriate recording equipment, can give time and distance information for various points along the line of flight. Using the experimental values of distance and time together with the theoretical work of the previous section, particle size and luminosity can be determined. The accuracy of the measurement depends upon the time and space resolution of the particle detectors.

In experiments with spray particles, the density of the ambient atmosphere becomes very important. Very small particles are decelerated extremely fast in a dense atmosphere and may travel less than a centimeter, whereas large particles in a rarefied atmosphere may not lose enough speed in a few meters to make deceleration measurements practical. Thus it is essential that the experimental work be carried out in a controllable atmosphere.

In a practical-sized laboratory vacuum tank, measurements can be made over a range of about 4 to 200 cm. Fig. 3 shows that over this range, size determinations can be made if $\alpha_o = C_D\rho/r_o\delta$ varies between

about 1.0 and 10 m^{-1}. To study a given size of particle, the value of density, ρ, must then be controlled such that α_o falls between these values.

Using this method of determining size and having a limited number of detectors, it is only possible to determine if a particle is or is not a certain size. As an example for the v_o and k values of Fig. 3, a particle whose size makes the quantity α_o equal to 10 m^{-1} can be measured if several detectors are placed in the distance range from about 5 cm to 15 cm from the target area. If $\alpha_o = 1.0\ m^{-1}$, the detection equipment would have to be placed about 50 to 150 cm from the target; if $\alpha_o = 100\ m^{-1}$, the range would be 0.05 to 0.15 cm. Thus, for a given positioning of the detection apparatus, the following information on particle size will be available: The particle is in a certain size range or the particle is larger than this size. It cannot be smaller, since a smaller particle will be decelerated rapidly and will not reach the detection equipment with sufficient velocity to be luminous.

Experimental Equipment

Vacuum Firing Range

Preliminary experimental studies of spray-particle dynamics were carried out in the vacuum firing range shown in Fig. 13. The tank is 6 x 1 x 1 ft. and is made of 1/2 in. steel plate. There are two large hatches on the top of the tank (shown by dotted lines) and five small openings, one at each end and three along the front face. Two 3/4 in.

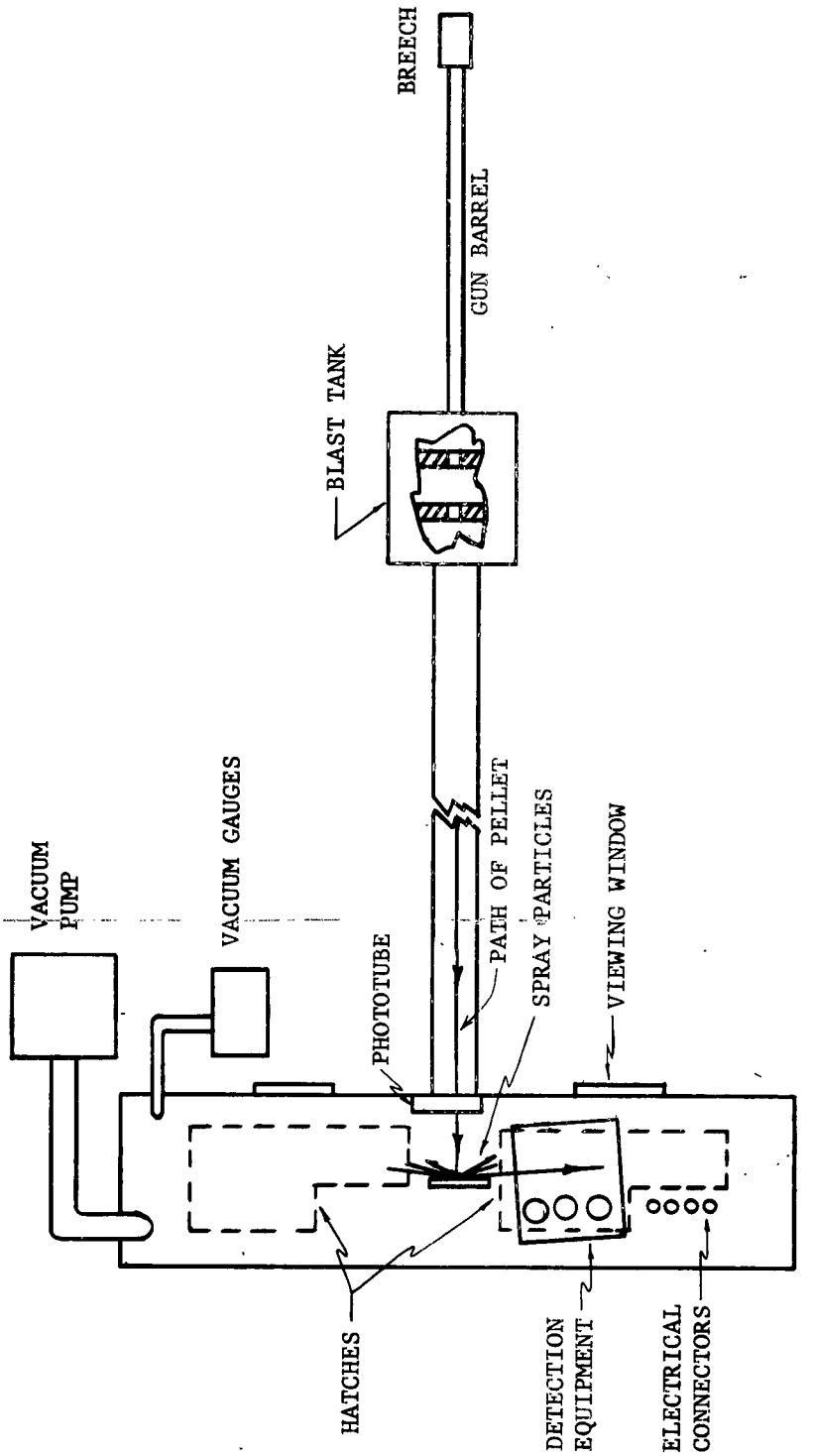

Fig. 13 Diagram of Vacuum Tank and Firing Range

aluminum plates are used for coverings for the hatches and are held down by screw clamps. Four of the small openings are covered with plexiglass for viewing purposes, and the fifth or center opening is connected through a blast tank to the gun.

The vacuum pump is a Welch Model 1403-B high vacuum pump, rated at 0.005 mm Hg ultimate pressure and a pumping speed of 100 liters per minute. It is connected to one end of the tank by a 3/4 in. metal pipe.

The pressure measuring apparatus consists of an oil manometer which reads down to approximately 10 cm Hg and a small mercury manometer reading down to 0.5 mm.

The gun used to accelerate the primary projectiles is mounted on a sturdy wooden table 15 feet from the main tank. The gun barrel consists of two 24 in. sections of 1-1/4 in. cylindrical steel stock containing a 22 caliber bore. One end of the barrel is chambered for a 220 swift cartridge. The gun is fired by means of a solenoid which forces the firing pin into the primer at the rear of the cartridge.

A blast tank is located at the forward end of the gun. It consists of a series of steel plates each containing a hole just slightly larger than the size of the pellet that is fired. These plates act as baffles which allow the pellet to pass unhindered, but show a high resistance to the powder gases following the pellet. The gases thus take longer to reach the target area than the pellet and do not interfere with the experiment.

A 4-1/2 in. diameter hollow pipe connects the blast tank to the center small opening on the front face of the main tank. This pipe

makes it possible to obtain a vacuum throughout the system, including the barrel of the gun, and also provides a shield in case the pellet does not travel straight down the range but careens off to one side.

Electrical connections can be made to equipment inside the tank by means of several coaxial connectors located at various positions on the top and a few general purpose connectors on the front face.

Spray Particle Detection Equipment

The luminosity of spray particles in an atmosphere makes it possible to use light-sensing devices for particle detection. The present equipment uses three photomultiplier tubes and associated circuitry to detect a high-speed particle as it passes and to give an output proportional to the luminous intensity. Figure 14 shows a circuit diagram for one of the three identical photomultiplier-tube detectors. The photomultiplier tube is an RCA Type 931-A which has a maximum current amplification of 800,000 using a voltage difference of 1000 volts d-c between anode and cathode and 100 volts between dynodes. An additional gain of 3 is proveded by a one-stage amplifier. A cathode follower matches the output impedance to that of the coaxial cable used to transmit the detection information to equipment outside the vacuum tank.

Three photomultiplier tubes are mounted in a straight line and placed in a rectangular aluminum box. The box serves as a light shield and holdsthe detectors securely positioned.

The distances between photomultiplier tubes, and from the first one to the front end of the box, are known to within 0.1 mm. At the

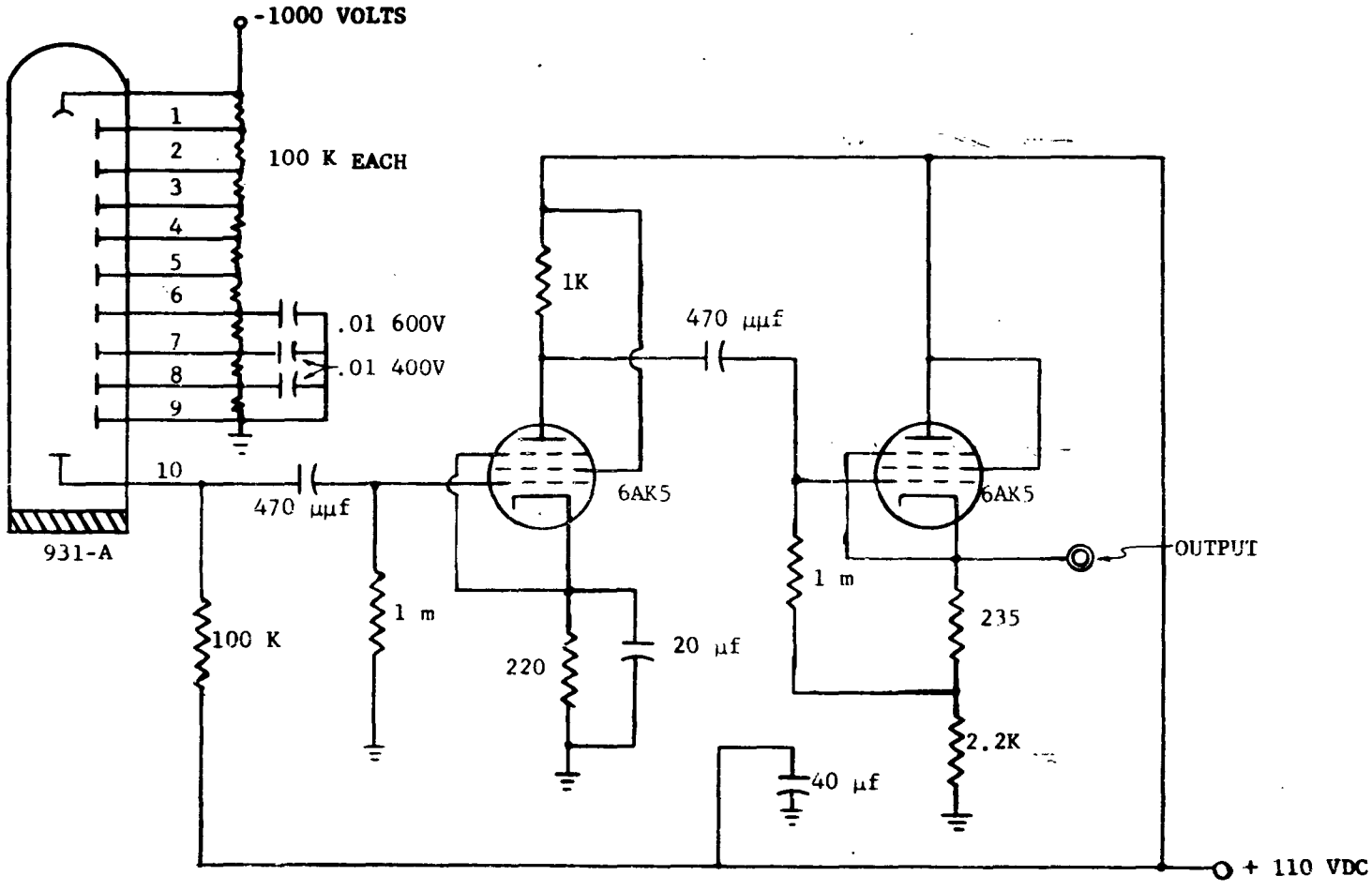

Fig. 14 Circuit diagram of spray particle detector

front end of the box a double wall serves as a shield to limit the number of particles entering the box. The wall sections are 3/8 in. apart and each contains a small hole. Spray particles traveling in a horizontal plane and in a position to pass the photomultiplier tubes will pass through the double hole and be detected.

It is desired that a given detector responds only when a particle passes directly in front of it. To restrict the field of view, a cylindrical aluminum cover shield containing a 1/4 inch slot is placed over the photomultiplier. A plane shield with an adjustable slit is placed immediately in front of the slot in the cover. With the variable slit adjusted to 0.5 mm and positioned 1.0 cm from the face of the photomultiplier, the viewing angle is approximately 3°. With this small angle of view, the particle will be detected as it travels a distance of 0.6 mm. The ideal angle of view is, of course, 0°, but as the slit is made narrower, light intensity is reduced and detection becomes difficult. Figure 15 is a photograph showing the particle-detection equipment.

A block diagram of the experimental arrangement can be seen in Fig. 16. Each of the three photomultiplier circuits is connected by means of coaxial cable to the vertical input of an oscilloscope. A phototube mounted above the target area views the flash occurring at impact and sends a triggering pulse simultaneously to the three oscilloscopes. Outputs of the detectors are displayed on the oscilloscope screens and photographed with a Dumont oscilloscope camera. Three points on a distance-versus-time plot for the particles are then known.

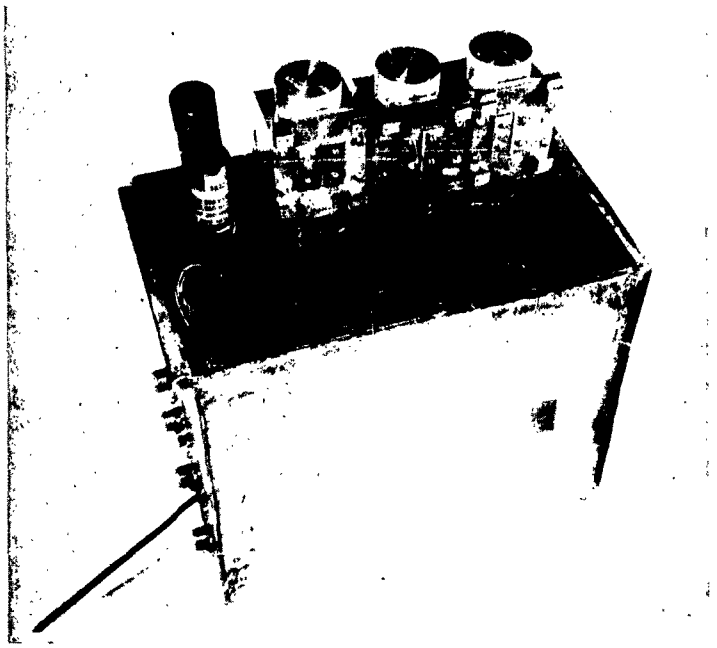

(a)

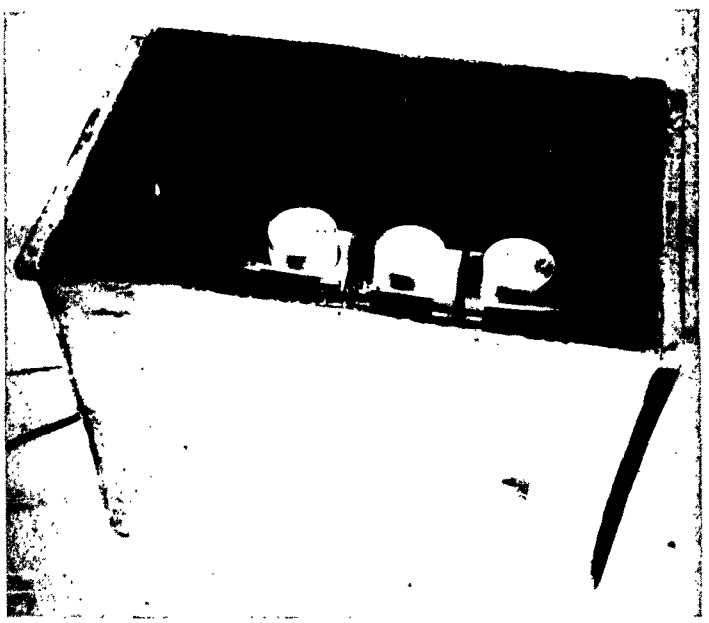

(b)

Fig. 15 Photographs showing spray particle detection equipment. Photomultiplier tubes and mounting board (a) outside of box; (b) in position inside box.

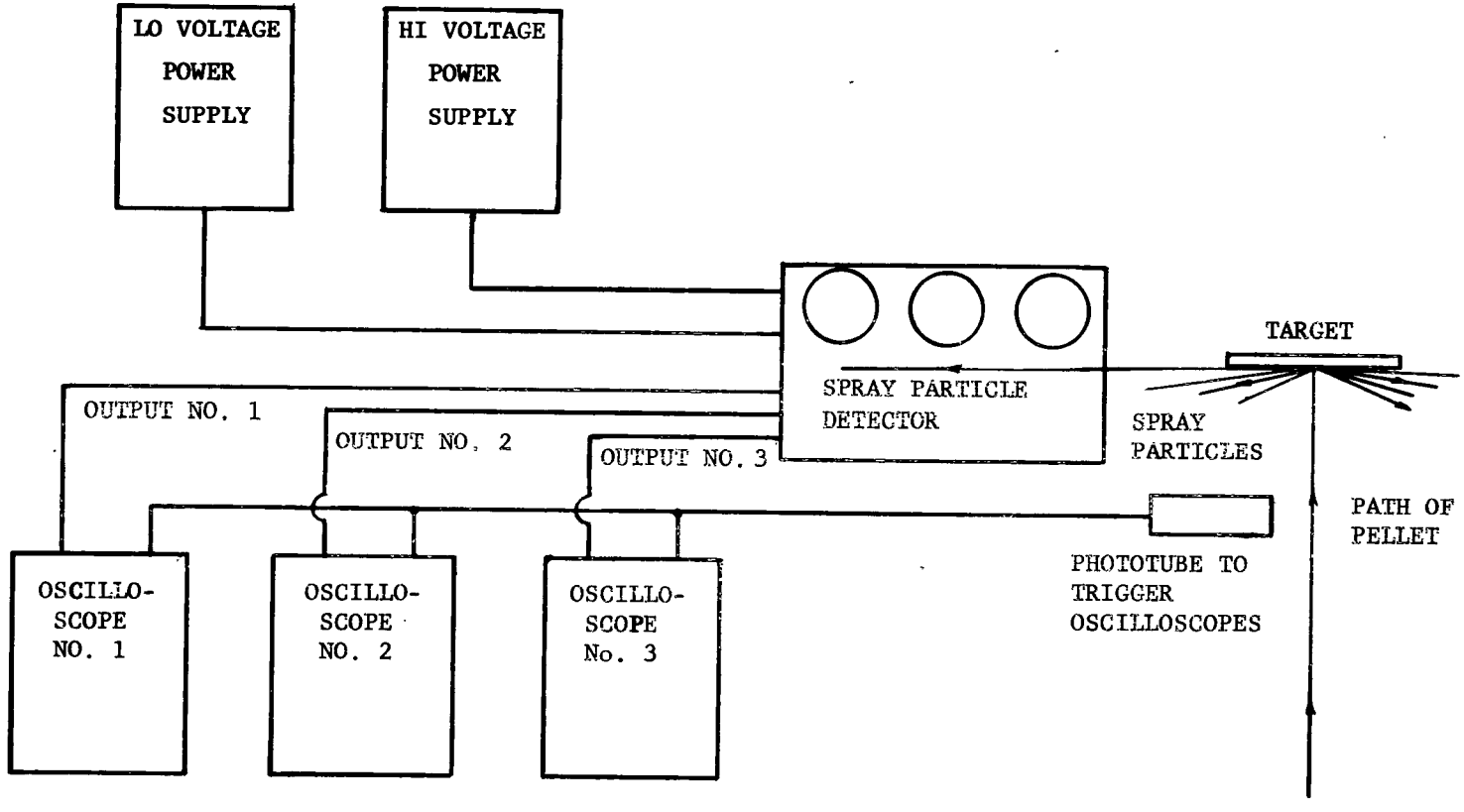

Fig. 16 Block diagram of spray particle detection equipment

Preliminary Experiments and Results

Preliminary experimental work was done using the vacuum system and firing range described. The detector box was positioned in the vacuum tank as shown in Fig. 13. The tests were made with 7/32 in. steel balls shot into a flat steel target. The detector box was placed so that the input holes were lined up approximately in the plane of the target and at right angles to the path of the primary projectile. It was found in earlier particle work[9] that the highest velocity spray comes off at very shallow angles to the plane of the target.

The first successful operation of the complete detection system resulted in the data shown below. The pressure in the tank was 1.5 cm Hg.

Photomultiplier	x cm	Shot 1 t (μ sec)	Shot 2 t (μ sec)	Shot 3 t (μ sec)
1	12.8	15	17	13
2	18.5	25	36	25
3	27.1	37	>50	38

	Shot 1	Shot 2	Shot 3
Average velocity between origin and tube 1	8.5 km/sec	7.5 km/sec	9.8 km/sec
Average velocity between tubes 1 and 2	5.7	2.8	4.3
Average velocity between tubes 2 and 3	4.7	<4.0	4.3

Oscilloscope traces of a typical shot are shown below. The data above are actually for a cloud of spray particles and not for a single particle. This is so because the input holes were 1/4 in. in diameter and permitted many particles to enter.

Traces are from right to left.

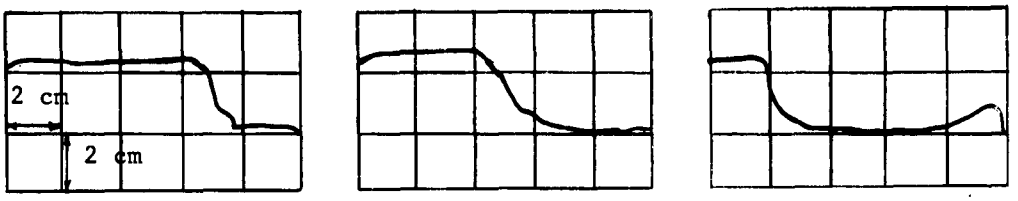

Output 1 Output 2 Output 3

2 volts/cm 5 μsec/cm

For a possible estimate of the size and velocity of the particles, the results of shot 3 were compared with the theory presented in Section II. From Fig. 4, it was found that the three experimentally determined points lie approximately on the curve for v_o = 15 km/sec and $\alpha_o = C_D\rho/r_o\delta = 10\ m^{-1}$. With C_D equal to 2.0, δ equal to 7.8 g/cm^3, and ρ equal to 2.4×10^{-5} g/cm^3 which corresponds to a pressure of 1.5 cm Hg, r_o is calculated to be 0.62×10^{-6} m. This result, although not exact since the data are for a cloud of particles and not an individual one, agrees with the size and velocity estimates of earlier work.[8,9] In a cloud of particles the large, initially slower particles overtake and pass the small, initially faster ones. Over long distances this would have to be considered; however, over the range of detection for the data listed above, the effect is probably unimportant. Thus, the leading edge of the cloud is made up of particles of nearly uniform size and velocity. From Fig. 2, it is found that particles with an initial velocity of 15 km/sec are reduced in size to 32%, 28%, and 26% of their original radius at the time they pass the first, second, and third photomultiplier tubes,

respectively. Little can be determined concerning luminosity because of the unknown number of particles that were detected.

The input holes were then made smaller to obtain fewer particles. An estimate of the actual number of particles being detected was made by using a microscope to count the number of craters produced in a highly polished target placed directly following the third photomultipiier tube. With 2 mm diameter shield holes, about 50 craters were observed. The fact that a group of 50 particles can be easily seen is of great interest in indicating that a single particle could be detected under similar conditions with only slight improvements in the light gathering capabilities of the detectors.

At this stage of the experimental work the old vacuum tank was abandoned and work begun on a new system.

Design of a New Vacuum Firing Range

With experience, it became evident that the vacuum range used in the first experiments was inadequate for single-particle studies. The main difficulty was that the pressure in the system could not be reduced enough to allow small, fast particles to reach the detectors. A second difficulty was that limited space prevented the most advantageous placement of detectors and alignment was difficult. To overcome these limitations, a new vacuum range was designed and is now nearing completion.

A top view of the new system appears in Fig. 17. The main tank is 4 ft. in diameter and 23 in. deep. The lid is a large circular piece of steel plate braced with crossed I-beams on the top. It is positioned on the tank by means of a counterweight and pulley system. Seven ports around the sides of the tank can be used for various purposes. A series of 5 ft. lengths of 10 in. diameter iron pipes is connected to one of the ports. The gun described in the discussion of the old system fires through these large-diameter pipes and into thelarge main tank. An aluminum plate containing a 1 in. hole at its center is placed between each section of pipe. This series of plates acts as a baffle to slow the gases that follow the pellet down the range. Electrical connections can be made to a number of hermatically sealed connectors mounted on an aluminum plate bolted to one of the large ports.

The vacuum equipment consists of a Stokes Model 212H-10 vacuum pump powered by a 5 hp, 220 volt-3 phase motor. The pump is rated at 0.010 mm Hg ultimate pressure, with a pumping speed of 140 cubic feet per minute. The vacuum connection to the tank is made with 3 inch copper tubing through a 3 inch gate valve. Pressure in the tank is measured with a Kinney Type T.D.-1 McCloud vacuum gauge.

The tank has adequate space for positioning detection equipment to measure particles leaving the target at any angle. Extension tubes can be placed on the large ports for long-range measurements. Tests show that pressures down to 0.1 mm Hg are easily obtained which should allow the observation of small particles traveling at higher velocities

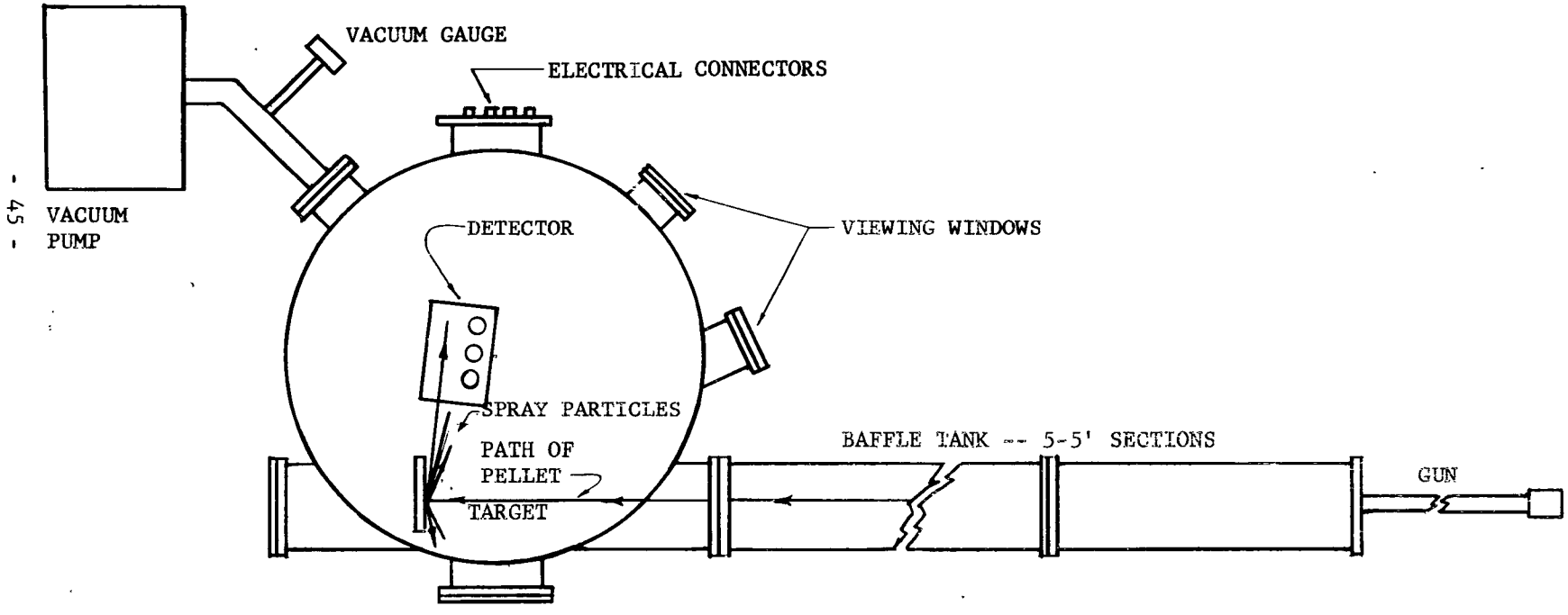

Fig. 17 Diagram of new vacuum tank and firing range

than in the first system.

A Proposed Experiment in the New Vacuum Range

With the theoretical background of Section II and the experience gained in the first experiments, a proposal for an experiment to utilize the capabilities of the new vacuum firing range can be made.

The first efforts will have to be directed toward obtaining a single spray particle, since the theoretical studies were made for one particle. It appears that the simplest way to do this is to reduce the size of the input holes to the detector. As the holes are made smaller, the problem of alignment of the detection equipment will be increased and the probability of getting a suitable particle will be decreased. Construction of a precision positioning device may help to solve this problem. It will be assumed for the discussion to follow that it is possible to obtain a single particle.

If the old detector box with its fixed spacing is used, it should be placed so that the first photomultiplier tube is approximately 5 cm from the target. Referring back to Fig. 2, it can be seen that 5 cm to 15 cm is the range in which the curve for a particle whose size makes α_o equal to 10 m^{-1}. The shot is made and the detector outputs, as photographed by the oscilloscope cameras, are studied and the experimental distance versus time values compared with the theoretical values. It can then be determined if the particle was in the desired size range or if it was larger. If it was in the desired size range, closer comparison with the theoretical curves will disclose the actual

size. A target placed in the spray particle path can be examined to see that only one particle was observed.

A number of refinements to the detection equipment will be suggested here. First, the detector box should be made larger and more photomultipliers added. Two photomultipliers are needed very close to the target area to measure initial velocity accurately. Another photomultiplier in the size measuring range would give more accuracy in plotting the trajectory curve.

Another refinement for the detection system would be to install a lens system in front of each photomultiplier tube to collect more light and focus it on the most sensitive spot of the tube. The lens system could consist of one simple lens with the proper focal length and could increase the amount of light reaching the detector by almost 100 times. This light gathering system may be necessary to successfully detect one particle, since its intensity will be very low.

Studies should be made of the effects on spray particle production of varying the impact angle. This might ~~be done~~ by ~~rotating the target~~ or by positioning the detection equipment at various angles to the face of the target.

If k (See Eq. 10, Section II) can be measured separately or by careful time-distance measurements of a spray particle, the luminous efficiency τ_o of Eq. 17 can be determined. This would be of great importance to meteor physics.

In the event that experimental difficulties prove too great to obtain a single particle, a cloud of spray particles could be studied to

yield much useful information about meteors. A spectrographic study of the light emitted would be of value.

IV. CONCLUSIONS

Equations for deceleration, size, time rate of change of mass, and luminosity can be written in terms of experimentally measurable quantities for a high-velocity particle moving in a controlled atmosphere. A digital computer can be used effectively to obtain solutions to the equations.

Many important observations can be made from a consideration of the solutions to the equations. It appears that it is possible to determine the size of spray particles by experimentally measuring their time of flight to given fixed distances. If the size of a particle is known, its luminosity can be calculated and compared with experimental results to determine the validity of the assumed luminosity equation. If the equation is found to hold, a value for τ, the luminous efficiency can be determined.

Experimental problems may prove to be great. It will be difficult to obtain a single spray particle, and if it is obtained, its luminous intensity may be so low that detection will be very difficult; however, detection should be possible for many cases of interest.

Spray particles provide one of the best, if not the only, means of studying meteor physics in the laboratory.

APPENDIX I

A SOLUTION OF THE EQUATIONS OF MOTION

Equation (11) is an expression for the deceleration of an ablating particle.

$$\frac{dv}{dt} = -\frac{3}{8}\frac{C_D\rho}{r_o\delta} v^2 e^{-k(v^2 - v_o^2)} \tag{11}$$

$\frac{dv}{dt}$ can be written as $v\frac{dv}{ds}$, so that

$$v\frac{dv}{ds} = -\frac{3}{8}\frac{C_D\rho}{r_o\delta} v^2 e^{-k(v^2 - v_o^2)} \tag{a}$$

Let $u = kv^2$ and $u_o = kv_o^2$, then

$$\frac{du}{ds} = 2kv\frac{dv}{ds} \tag{b}$$

and

$$\frac{dv}{ds} = \frac{1}{2kv}\frac{du}{ds} \tag{c}$$

Substituting the value for u and combining equations (a) and (c)

$$\frac{du}{ds} = -\frac{3}{4}\frac{C_D\rho}{r_o\delta} ue^{-(u - u_o)} \tag{d}$$

Rearranging

$$\frac{e^{u - u_o}}{u} du = -\frac{3}{4}\frac{C_D\rho}{r_o\delta} ds \tag{e}$$

Equation (e) can be integrated to obtain distance as a function of velocity.

$$e^{-u_o} \int_{u_o}^{u} \frac{e^u}{u}\, du = -\frac{3}{4}\,\frac{C_D\rho}{r_o\delta}\,(s - s_o) \qquad (f)$$

where s_o is the initial displacement at $v = v_o$. The integral in Eq. (f) may be separated into two parts as follows:

$$\int_{-\infty}^{u} \frac{e^u}{u}\, du - \int_{-\infty}^{u_o} \frac{e^u}{u}\, du = -\frac{3}{4}\,\frac{C_D\rho}{r_o\delta}\, e^{u_o}(s - s_o) \qquad (g)$$

Values are tabulated for exponential integrals of the type appearing on the left side of Eq. (g).[17] Using the conventional symbol for the exponential integral and substituting for u and u_o, Eq. (g) becomes

$$Ei(kv^2) - Ei(kv_o^2) = -\frac{3}{4}\,\frac{C_D\rho}{r_o\delta}\, e^{kv_o^2}\,(s - s_o) \qquad (h)$$

Similar equations were derived by Hoppe[3] and Hansen[5] for a meteor moving in an atmosphere of exponentially increasing density.

APPENDIX II

COMPUTER PROGRAM FOR SOLVING THE EQUATIONS OF MOTION

The Datatron 205 digital computer was programmed to solve the following set of linear first order differential equations for velocity and displacement.

$$\frac{dv}{dt} = -\frac{3}{8}\,\frac{C_D \rho}{r_o \delta}\, v^2\, \epsilon^k\, (v_o^2 - v^2)$$

$$\frac{ds}{dt} = v$$

with the initial conditions, $s_o = t_o = 0$.

The program also provides for the solution to the following equations:

$$\frac{r}{r_o} = e^k\, (v^2 - v_o^2)$$

$$\frac{1}{r_o^2 C_D \rho}\,\frac{dm}{dt} = -3\pi k \left(\frac{r}{r_o}\right)^2 v^3$$

$$\frac{1}{r_o^2 C_D \rho}\,\frac{I}{\tau_o} = -\frac{1}{2}\left[\frac{1}{r_o^2 C_D \rho}\,\frac{dm}{dt}\right] v^3$$

Values for the various equation parameters were put on cards as shown.

WORD 1	WORD 2	WORD 3	WORD 4	WORD 5	WORD 6	WORD 7	WORD 8
k	C_D	ρ	r_o	δ	v_o		ID No.

A new card can be punched when solutions are desired for any particular set of parameters.

The program, sub-routines, and parameter values are stored in the memory as follows:

Memory Locations	
0000-0198	differential equation sub-routine (2.50.010)
0360-0479	program
1010-1019	parameters
2000-2109	ϵ^x sub-routine (2.20.120)
6000-6109	data for diff. eq. sub-routine

The program is coded as follows:

MAIN	BAND	INSTRUCTION			
Start with 30 0390					
0360	7360	0	0000	34	1000
1	1			64	5001
2	2			02	4002
3	3			64	5001
4	4			82	5001
0365	7365			02	6005

0366	7366	0	0000	64	4015
7	7			82	4015
8	8			81	6005
9	9			82	4010
0370	7370			20	0371
1	1			31	2000
2	2			30	0373
3	3			82	6005
4	4			02	6006
0375	7375			64	7019
6	6			82	4011
7	7			82	4012
8	8			30	0380
9	9	1	5037	50	0000
0380	7380	0	0000	83	4013
1	1			83	4014
2	2			82	6006
3	3			02	4001
4	4			64	7019
0385	7385			81	5001
6	6			05	7009
7	7			64	5000
8	8			02	6003
9	9			20	0171
0390	7390	0	9990	44	1010
1	1	0	9980	54	8010
2	2	0	0000	64	4015
3	3			02	0201
4	4			02	0200
0395	7395			02	0202
6	6			64	6019
7	7			02	6003
8	8			30	0440
9	9	0	5150	00	0000
0400	7400	0	0000	24	0420
1	1			02	6013
2	2			34	1000
3	3			64	4015
4	4			82	4015
0405	7405			02	6008
6	6			64	0201
7	7			82	0201
8	8			81	6008
9	9			82	4010
0410	7410			20	0411
1	1			31	2000

```
0412      7410      0  0000  30  0413
   3         3               12  0203
   4         4               12  6007
0415      7415               82  6007
   6         6               02  6007
   7         7               30  0460
   8         8               00  0000
   9         9               00  0000

0420  --  0439      (Used for blocking)

0440      7440      0  0000  64  7019
   1         1               02  6002
   2         2               30  0000

0459                0  4510  00  0000

0460      7460      0  0000  64  0201
   1         1               12  6005
   2         2               82  6005
   3         3               82  6005
   4         4               82  6007
0465      7465               82  4010
   6         6               82  7019
   7         7               12  0204
   8         8               82  6005
   9         9               82  6005
0470      7470               82  6005
   1         1               82  7018
   2         2               02  0205
   3         3               34  0420
   4         4               30  0006
0475      7475               00  0000
   6         6               00  0000
   7         7               00  0000
   8         8            1  5050  00  0000
   9         9            1  5194  24  7780
```

1010	4010	K
1	1	C_D
2	2	ρ
3	3	r_o
4	4	δ
1015	4015	V_o
6	6	blank
7	7	ID No.
8	8	blank
9	9	blank

6000	0	0000	00	0001
1	0	0000	00	0001
2	0	4510	00	0000
3	0	9999	99	9999
4	0	4710	00	0000
6005		(zero)		
6		(zero)		
7		(zero)		
8		(zero)		
9	0	0000	00	0002
6010	0	0000	10	0000
1	0	0000	00	0001
2	0	5140	00	0000
3		(zero)		
4		(zero)		
6015	0	5110	00	0000
6	0	5050	00	0000
7	0	5120	00	0000
8	0	5160	00	0000
9	0	9999	99	9999

VI. REFERENCES

1. E. J. Öpik, Tartu Observatory Publication, 25, No. 1, Finland, (1922).

2. F. A. Lindemann and G. M. B. Dobson, "A Theory of Meteors and the Density and Temperature of the Outer Atmosphere to Which It Leads." Proc. Roy. Soc. of London, Series A, 102, January 1, 1923.

3. J. Hoppe, "Die Physikalischen Vorgange beim Eindringen Meteorische Korper in die Erdatmosphare," Astron. Nachr., 262, (1937).

4. F. L. Whipple, "Meteors and the Earth's Upper Atmosphere," Rev. Mod. Phys., 15, 252, (1943).

5. C. F. Hansen, The Erosion of Meteors and High-Speed Vehicles in the Upper Atmosphere, National Advisory Committee for Aeronautics, Technical Note 3962, March 1957.

6. E. J. Öpik, Physics of Meteor Flight in the Atmosphere, Interscience Publishers, Inc., New York, 1958.

7. B. J. Levin, The Physical Theory of Meteors and Meteoric Matter in the Solar System, Moscow, 1956.

8. W. H. Clark, R. R. Kadesch, and R. W. Grow, Hypervelocity Impact Spray Particles, Technical Report No. OSR 18, Contract No. AF 49(638)-462, Department of Electrical Engineering, University of Utah, May 1960.

9. R. E. Blake, R. W. Grow, and E. P. Palmer, Velocity and Size Distribution of Impact Spray Particles, Technical Report No. OSR-19, Contract No. AF 49(638)-462, Department of Electrical Engineering, University of Utah, May 1960.

10. A. F. Cook, "The Physical Theory of Meteors VI the Light Curve," Astrophys. J., 120, 572, (1954).

11. E. J. Öpik, "Research on the Physical Theory of Meteor Phenomena III." Publications de L'Observatoire Astronomigre de L'Universite de Tartu, Finland, Tome XXIX, No. 5, 1937.

12. R. M. L. Baker, Jr., "The Iransitional Aerodynamic Drag of Meteorites," Astrophysical Journal, 129, 826 (1959).

    ----------"Effect of Accommodation on the Transitional Aerodynamical Drag of Meteorites," Astrophysical Jour., 130, 1024 (1959).

    ----------"Sputtering as it is Related to Hyperbolic Meteorites," Jour. Appl. Physics, 30, 550 (1959).

    ----------and A. F. Charwat, "Transitional Correction to the Drag of a Sphere in Free-Molecule Flow," Physics of Fluids, 1, 73 (1958).

13. M. A. Cook, H. Eyring, and R. N. Thomas, "The Physical Theory of Meteors. I. A Reaction-Rate Approach to the Rate of Mass Loss in Meteors," Astrophys. J., 113, 475 (1951).

14. G. L. Wehner, "Controlled Sputtering of Metals by Low-Energy Hg. Ions," Phys. Rev., 102, 690 (1956).

15. J. S. Clark, R. R. Kadesch, and R. W. Grow, Spectral Analysis of the Impact of Ultra Velocity Copper Spheres Into Copper Targets, Technical Report No. OSR-16, Contract No. AF 18(600)-1217, Electrical Engineering Department, University of Utah, September 1959.

16. R. W. Grow, R. R. Kadesch, E. P. Palmer, W. H. Clark, J. S. Clark, and R. E. Blake, "Experimental Investigation of Spray Particles Producing the Impact Flash," Proceedings of the Fourth Symposium on Hypervelocity Impact, Eglin Air Force Base, Florida, September 1960.

17. Tables of Sine, Cosine, and Exponential Integrals, US Work Projects Administration, New York City, 1940, 2 v.

DISTRIBUTION LIST

Agency	No. of Copies
Commander Air Force Office of Scientific Research ATTN: SRLT Washington 25, D. C.	2
P. O. Box AA Wright-Patterson Air Force Base Ohio	1
U. S. Atomic Energy Commission Technical Information Extenstion P. O. Box 62 Oak Ridge, Tennessee	1
Director Department of Commerce Office of Technical Services Washington 25, D. C.	1
Commander AF Ballistic Missile Division ATTN: WDSOT AF Unit Post Office Los Angeles 45, California	1
Commanding General U. S. Army Signal Corps Research Development Laboratory ATTN: SIGFM/EL-RPO Ft. Monmouth, New Jersey	1
National Aeronautics and Space Administration Washington 25, D. C.	6
Advanced Research Projects Agency Washington 25, D. C.	1
Director Air University Library AUL 9663 Maxwell Air Force Base Alabama	1
Chairman Canadian Joint Staff For DRB/DSIS 2450 Massachusetts Ave. N. W. Washington 25, D. C.	1

Agency	No. of Copies
Commander Air Force Office of Scientific Research Air Research and Development Command ATTN: SRYP Washington 25, D. C.	3
Commander Wright Air Development Center ATTN: WCOSI-3 Wright-Patterson Air Force Base, Ohio	4
Commander Air Force Cambridge Research Center ATTN: CROT L. G. Hanscom Field Bedford, Massachusetts	1
Commander Air Force Cambridge Research Center ATTN: W. G. Chase CRZCM L. G. Hanscom Field Bedford, Massachusetts	1
Commander Rome Air Development Center ATTN: RCSST-4 Griffiss Air Force Base Rome, New York	1
Commander European Office Air Research and Development Command 47 rue Cantersteen Brussels, Belgium (Air Mail)	2
Commander ASTIA ATTN: TIPDR Arlington Hall Station Arlington 12, Virginia	10
Director, Office of Naval Research Chicago Branch Office 86 East Randolph Street Chicago 1, Illinois	1

Agency	No. of Copies
Chief of Naval Research Department of the Navy ATTN: Code 420 Washington 25, D. C.	1
Commander Air Research and Development Command ATTN: RDR Andrews Air Force Base Washington 25, D. C.	1
Commander Air Research and Development Command ATTN: RDRR Andrews Air Force Base Washington 25, D. C.	1
Commander Air Research and Development Command ATTN: RDSFI Andrews Air Force Base Washington 25, D. C.	2
Director of Research and Development Headquarters USAF ATTN: AFDRD Washington 25, D. C.	1
Commander Air Force Special Weapons Center ATTN: Technical Library Kirtland Air Force Base, New Mexico	1
Commanding Officer Aberdeen Proving Ground ATTN: WSL Aberdeen, Maryland	1
Commander Frankford Arsenal ATTN: Director, Pitman-Dinn Laboratories Philadelphia 37, Pa.	1
Commander Air Force Armament Center ATTN: Technical Library Eglin Air Force Base, Florida	1

Agency	No. of Copies
Commanding Officer Picatinny Arsenal ATTN: Technical Division Dover, New Jersey	1
Chief, Bureau of Ordnance Research and Development Division Department of the Navy Washington 25, D. C.	1
Commander Armament Division Air Proving Ground Center ATTN: ACRG Eglin Air Force Base, Florida	1
Commandant USAF Institute of Technology ATTN: Technical Library MCLI Wright-Patterson Air Force Base, Ohio	1
Director, Naval Research Laboratory ATTN: Technical Information Officer Washington 25, D. C.	1
Director, Research and Development Division General Staff Department of the Army Washington 25, D. C.	1
Chief, Physics Branch, Division of Research U. S. Atomic Energy Commission 1901 Constitution Avenue, NW Washington 25, D. C.	1
National Bureau of Standards Library Room 203, Northwest Building Washington 25, D. C.	1
National Science Foundation 1520 H Street, N. W. Washington 25, D. C.	1
Director, Office of Ordnance Research Box CM, Duke Station Durham, North Carolina	1

Agency	No. of Copies
Commanding Officer U. S. Naval Ordnance Test Station ATTN: Earl B. Mayfield China Lake, Califqrnia	2
Commander Air Force Ballistic Missile Division Air Research and Development Command ATTN: WDTLAR Inglewood, California	1
Commander Air Force Flight Test Center ATTN: Technical Library Edwards Air Force Base, California	1
Commander Wright Air Development Center ATTN: WCLGO-1 Wright-Patterson Air Force Base, Ohio	1
Commander Air Force Missile Development Center ATTN: Technical Library Holloman Air Force Base, New Mexico	1
Commander Army Rocket and Guided Missile Agency ATTN: ORDXR-OTL Redstone Arsenal, Alabama	1
Institute for Air Weapons Research Museum of Science and Industry University of Chicago Chicago 37, Illinois	1
Armour Research Foundation 10 West 35th Street Chicago 16, Illinois ATTN: K. Miller	1
Rand Corporation ATTN: Dr. J. H. Huth ATTN: Librarian 1700 Main Street Santa Monica, California	1
Dr. P. Whitman Applied Physics Laboratory Johns Hopkins University Silver Spring, Maryland	1

Agency	No. of Copies
Pennsylvania State University ATTN: Dr. Davids University Park, Pa.	1
Utah Research and Development Co., Inc. 1820 S. Industrial Road Salt Lake City 4, Utah ATTN: Dr. W. S. Partridge	1
Dr. H. I. Leon Ramo Wooldridge Corp. 8820 Bellanea Ave. Los Angeles 45, California	1
Commanding Officer Aberdeen Proving Ground ATTN: Terminal Ballistic Laboratory Aberdeen, Maryland	1